Accepted Manuscript

Diagenetic control on mineralogical suites in sand, silt, and mud (Cenozoic Nile Delta): Implications for provenance reconstructions

Eduardo Garzanti, Sergio Andò, Mara Limonta, Laura Fielding, Yani Najman

PII:	S0012-8252(18)30139-9
DOI:	doi:10.1016/j.earscirev.2018.05.010
Reference:	EARTH 2631
To appear in:	*Earth-Science Reviews*
Received date:	4 March 2018
Revised date:	13 April 2018
Accepted date:	9 May 2018

Please cite this article as: Eduardo Garzanti, Sergio Andò, Mara Limonta, Laura Fielding, Yani Najman , Diagenetic control on mineralogical suites in sand, silt, and mud (Cenozoic Nile Delta): Implications for provenance reconstructions. The address for the corresponding author was captured as affiliation for all authors. Please check if appropriate. Earth(2017), doi:10.1016/j.earscirev.2018.05.010

Diagenetic control on mineralogical suites in sand, silt, and mud (Cenozoic Nile Delta): implications for provenance reconstructions

Eduardo Garzanti[a]*, Sergio Andò[a], Mara Limonta[a], Laura Fielding[b], Yani Najman[b]

[a]Laboratory for Provenance Studies, Department of Earth and Environmental Sciences, University of Milano-Bicocca, 20126 Milano, Italy

[b]Lancaster Environment Centre, Lancaster University, Lancaster, LA1 4YQ, U.K.

* Corresponding author: eduardo.garzanti@unimib.it

Abstract

This Nile Delta case study provides quantitative information on a process that we must understand and consider in full before attempting provenance interpretation of ancient clastic wedges. Petrographic and heavy-mineral data on partly lithified sand, silt, and mud samples cored from the up to 8.5 km-thick post-Eocene succession of the offshore Nile Delta document systematic unidirectional trends. With increasing age and burial depth, quartz increases at the expense of feldspars and especially of mafic volcanic rock fragments. Heavy-mineral concentration decreases drastically, transparent heavy minerals represent progressively lower percentages of the heavy fraction, and zircon, tourmaline, rutile, apatite, monazite, and Cr-spinel relatively increase at the expense mainly of amphibole in Pliocene sediments and of epidote in Miocene sediments. Recent studies have shown that the entire succession of the Nile Delta was deposited by a long drainage system connected with the Ethiopian volcanic highlands similar to the modern Nile since the lower Oligocene. The original mineralogy should thus have resembled that of modern Delta sand much more closely than the present quartzose residue containing only chemically durable heavy minerals. Stratigraphic compositional trends, although controlled by a complex interplay of different factors, document a selective exponential decay of non-durable species through the cored succession that explains up to 95% of the observed mineralogical variability. Our calculations suggest that heavy minerals may not represent more than 20% of the original assemblage in sediments buried less than ~ 1.5 km, more than 5% in sediments buried between 1.5 and 2.5 km, and more than 1% for sediments buried more than 4.5 km. No remarkable difference is detected in the intensity of mineral dissolution in mud, silt, and sand samples, which argues against the widely held idea that unstable minerals are prone to be preserved better in finer-grained and therefore presumably less permeable layers. Intrastratal dissolution, acting through long periods of time at the progressively higher temperatures reached during burial, can modify very drastically the relative abundance of detrital components in sedimentary rocks. Failure to recognize such a fundamental diagenetic bias leads to grossly mistaken paleogeographic reconstructions, as documented paradigmatically by previous provenance studies of ancient Nile sediments.

Keywords: Nile paleodrainage; Stratigraphic trends; Burial diagenesis; Grain-size control; Quartz durability; Transparent-heavy-mineral concentration; Intrastratal dissolution; Diagenetic minerofacies.

1. Introduction

The first question we need to ask when interpreting the detrital suite of an ancient sediment sample is whether and to what extent the observed mineralogical spectrum reflects the original composition at the instant of deposition. Does the assemblage chiefly reflect provenance or diagenesis? If the question remains unasked, then the risk is that we carry on under the assumption that what we see is "more or less" what the original composition was (Kahneman 2011). It has long been known that chemical dissolution of less durable grains operating through geological time during burial may be very extensive, able to modify progressively the detrital suite and to finally erase most provenance information (Bramlette, 1941; Pettijohn, 1941; Gazzi, 1965; Milliken et al., 1989). No mineral formed at high temperature within the crust is inert at the Earth's surface or in the shallow subsurface, and in the long run a sediment may be transformed into a strongly depleted residue composed of a few resistant minerals only, such as quartz, zircon, tourmaline, and rutile (Hubert, 1962; McBride, 1985). The hope is that although this may happen in porous and permeable sandstones, a wider spectrum of the original assemblage might be preserved in impermeable mudrocks or tightly cemented concretions formed early in diagenetic history (Blatt and Sutherland, 1969; Cibin et al., 1993). Despite all information obtained from heavy-mineral studies worldwide (Milliken, 2007; Morton and Hallsworth, 2007), these problems present new and often ambiguous aspects in any specific case, and the efforts spent in the search for solutions of general validity are inevitably baffled to some extent.

One useful approach to quantify diagenetic effects is to combine systematically petrographic and heavy-mineral observations with an accurate quantification of the amount of heavy minerals yielded by the sample (i.e., their absolute abundance or concentration; Garzanti and Andò, 2007a). If heavy minerals are abundant and unstable ferromagnesian minerals common, then chances are high that the suite is largely primary and chiefly reflects provenance. If heavy minerals are rare and represented by a narrow spectrum of predominantly durable species, then we should suspect a strong diagenetic effect in sediments even as young as the Plio-Pleistocene (Milliken, 1988).

Similar residual assemblages, however, may result also from recycling - which is the effect of chemical dissolution accumulated through a series of sedimentary cycles - or from extreme pre-depositional weathering conditions, and more in general from a combination of these different factors (Johnsson, 1993; Garzanti, 2017). A fruitful approach to solve the tangle is to analyze in detail the mineralogical trends recorded by a thick vertical succession deposited at the mouth of a large river system, for which provenance may be assumed, as a first approximation, as constant through time. If such a "steady state" assumption is at least broadly fulfilled, then the effect of burial diagenesis can be isolated and assessed.

One place exceptionally well suited to carry out such an investigation is the thick sedimentary succession accumulated since the lower Oligocene in the offshore Nile Delta (Craig et al., 2011). In this article, we compare the compositional signatures of Nile River and Nile Delta sediments - sampled both before and after the closure of the Aswan High Dam in 1964 and transported both as bedload and suspended load (Garzanti et al., 2006, 2015; Fielding et al., 2017) - with those of partly lithified Oligocene to Pleistocene Nile Delta sands, silts, and muds cored offshore by BP Egypt (Fig. 1; Fielding et al., 2018). The latter paper focuses principally on provenance, whereas the present one illustrates in full detail the stratigraphic trends shown by petrographic modes and heavy-mineral suites and thoroughly discusses their potential controlling factors. Here we dedicate specific attention to comparing heavy-mineral assemblages in loose sediments and consolidated sedimentary rocks ranging in grain size from cohesive mud to upper-medium sand, in order to evaluate differences in the intensity of diagenetic effects in strata characterized by different porosity and permeability to intrastratal fluids. In the final part of the article, we integrate our results with heavy-mineral data from extensively studied sedimentary basins worldwide - including the Gulf of Mexico, North Sea, and Bay of Bengal - and propose a standard sequence of mineralogical facies that may be used to investigate and sort out the relative impacts of provenance and diagenesis in the analysis of ancient clastic wedges.

2. The Nile since the Oligocene

As early as the fifth century B.C., the Greek historian Herodotus recognized that "*Egypt was the gift of the Nile*" and that its soil "*is black and friable as one would expect of an alluvial soil formed of the silt brought down by the river from Ethiopia*" (The Histories II, 5 and 12). The very name Egypt is derived from "*Gapt*", which in ancient language meant black soil (i.e., the fingerprint of Ethiopian volcanic province). But has this always been so? When did this begin?

2.1. The age of the Nile

The birth of a long Nile drainage system connecting equatorial and subequatorial Africa to the Mediterranean Sea across the hyperarid Sahara Desert has remained a very controversial issue for half a century and more. The ages proposed for the origin of a paleo-Nile sourced in the Ethiopian highlands range from as old as the Late Eocene (Underwood et al., 2013) to as recent as the last half Ma (Hassan, 1976; Issawi and Osman, 2008), whereas the White Nile is generally believed to have formed by overflow from Lakes Victoria and Albert even more recently (12.5 to > 250 ka; Salama, 1987; Williams et al., 2003).

On one side, researchers noted the youthful character of parts of the river course, namely the six cataracts between Khartoum and Aswan, and concluded that the making of the Nile did not begin before ~ 6 Ma ("Eonile" of Said, 1993) and that a long river connected with Ethiopia did not exist prior to 700-800 ka ("Prenile" of Said, 1993). Before the Messinian, when a deep canyon was incised across Egypt during the dramatic fall of Mediterranean sea level (Chumakov, 1968), supposedly triggering flow reversal by headward erosion and river capture, the main drainage was held to be southward in southern Egypt (Issawi and McCauley, 1992). Landform analysis has suggested that, before then, equatorial and sub-equatorial rift highlands drained largely toward the Atlantic Ocean via a "Trans-African drainage system" (McCauley et al., 1986) and paleo-Congo

(Talbot and Williams, 2009), or internally into the Sudd and other Sudanese rift basins (Salama, 1997). In this scenario, detritus at the Delta would have been supplied by a short stream sourced locally in the Red Sea Hills ("Paleonile" of Said, 1993; Macgregor, 2012). A most recent establishment of a long "Prenile" draining Ethiopian volcanic highlands was inferred by Shukri (1950 p.524-527), who in his pioneering heavy-mineral study of the Nile noted the great difference between clinopyroxene-rich recent sediments and Plio-Pleistocene sediments where augitic clinopyroxene is invariably absent or extremely rare. On this basis, he concluded (p. 512) that "*during the Pliocene and Plio-Pleistocene the Nile brought no sediments to Egypt comparable with those of the present tributaries draining the Abyssinian plateau, and that the Atbara and Blue Nile sediments reached Egypt in more recent times*". Augite-free heavy-mineral assemblages of Pliocene and Plio-Pleistocene sediments were held to be supplied by "*both the White Nile and lateral valleys in Egypt*" (Shukri, 1950 p.525).

Very differently, other researchers have claimed that an Ethiopian connection has existed since the Oligocene, originating from the early stages of East African rifting, magmatic upwelling, and associated topographic uplift of the Ethiopian highland region (Berry and Whiteman, 1968; McDougall et al. 1975; Adamson et al., 1993). Supporting arguments include large-scale geomorphological observations (Burke and Wells, 1989; Cox, 1989), thermochronological data and reconstruction of the incision history of the Blue Nile gorge (Pik et al., 2003; Gani et al., 2007), and tomography-based investigations of mantle convection (Moucha and Forte, 2011). Extensive information by seismic and drilling activities has recently established that terrigenous sedimentation in the offshore Nile Delta and submarine fan began in the early Oligocene, above a major unconformity correlating onshore to a sharp change from Eocene carbonates to the overlying channelized clastic rocks (Dolson et al., 2002, 2005). The mid-upper Oligocene succession is very thick and represented by sandy turbidites, deposited since ~ 30 Ma and overlain by rapidly prograding deltaic sediments since 27.5 Ma (fig. 31 in Craig et al., 2011). Nevertheless, mainly on the basis of mineralogical data supposedly suggesting diminishing relative

contributions from Ethiopia with increasing age, Macgregor (2012) concluded that before the Pliocene "*the largest sediment contributor was the Red Sea Hills*" and that "*Nubia was a significant supplier of sand-rich sediment during wet periods*". In contrast with this view, the multi-technique mineralogical, geochemical, and geochronological provenance analysis of the very same Nile Delta succession studied here has recently documented that the Ethiopian connection was established in the Oligocene (Fielding et al., 2018). One smoking gun is provided by the population of detrital zircons with U-Pb age ≤ 32 Ma, diagnostic of Ethiopian provenance (Fielding et al., 2017; Garzanti et al., 2018a), which is recorded in mid-Oligocene strata (27.5 Ma) and throughout the overlying Neogene succession (Fielding et al., 2018). The fundamental premise of the present study, i.e., that a long Nile River sourced in Ethiopian volcanic rift highlands has existed since the Oligocene, is therefore considered as robust.

2.2. The Nile in the Quaternary

The lively debate between opposite views about the recent *versus* ancient origin of the Nile reveals how the available information is not solid enough to develop a thorough understanding of the pre-Quaternary evolution of the Nile river system. Only a tentative piecemeal reconstruction of potential paleotectonic (Pik et al., 2003; Gani et al., 2009; Sembroni et al., 2016) and paleoclimatic scenarios (Griffin, 2002; Pickford et al., 2006; Sepulchre et al., 2006; Abdelkareem et al., 2012) is possible at present. The Quaternary, and especially the late Quaternary history of the Nile, is far better constrained (Woodward et al., 2015). Marked variations in water discharge controlled by climatic change and temporary disconnection from the Victoria, Albert, and Turkana Lakes of Uganda have been reconstructed and dated with notable accuracy for the White Nile (Williams and Talbot, 2009), and shown to coincide temporarily with Blue Nile flood events in the last 15 ka at least (Williams, 2009). Nile flood events have been documented to be synchronous with deposition of dark organic muds in the eastern Mediterranean basin during the last 124 ka

(sapropel units S5-S1) with more uncertain links with sapropel units as old as 240 ka (S9-S6), thus highlighting the close causal relationship between astronomic precession cycles, intensification of the summer monsoon, Nile water fluxes, and sedimentation in the Mediterranean Sea (Williams et al., 2015).

Very marked fluctuations in water discharge controlled by climate change must have corresponded to even larger fluctuations in the sediment flux, eventually amplified by human intervention in the last thousands of years (Nyssen et al., 2004, 2008). In the last half century, estimates of Nile sediment load have increased from 57 10^6 t a^{-1} (Hurst, 1957), to 108 ± 5 10^6 t a^{-1} (Summerfield and Hulton, 1994; Hay, 1998), and to 230 ± 30 10^6 t a^{-1} (corresponding to sediment yields of 800 ± 150 t km^{-2} a^{-1} and erosion rates of 0.29 ± 0.05 mm a^{-1} in the Ethiopian highlands; Garzanti et al., 2006), which suggests anthropically accelerated erosion caused by deforestation and intensive land use by a rapidly expanding population. Cosmogenic ^{10}Be measurements on quartz from beach sample S3289 collected from the Damietta deltaic cusp (N31°29'22" E31°46'47") point to catchment-wide erosion rates of 0.026 ± 0.002 mm a^{-1} averaging over millennial time scales (H.Haedke and H.Wittmann, pers. comm. 2017). This value matches well the estimated present sediment flux of 230 10^6 t a^{-1}, corresponding to a sediment yield of 77 t km^{-2} a^{-1} and to an average erosion rate of 0.028 mm a^{-1} calculated over the entire huge catchment area of 3 10^6 km^2.

Three main components can be identified for modern Nile and Nile Delta sediments: a) volcanic detritus derived from Ethiopian highlands, dominant in levees and fluvial bars of the Atbara River, and in levees of the Blue Nile and the main Nile; b) detritus derived from Neoproterozoic ("Pan-African") crystalline basement exposed all along the Red Sea rift shoulder, representing a large fraction of Blue Nile and main Nile fluvial bars; and, c) detritus recycled from Phanerozoic cover strata, which characterizes ephemeral tributaries of the lower course draining either the Red Sea Hills or the Sahara metacraton and dune sands of the Western Desert. The vast White Nile catchment does not represent a significant sediment source, because detritus generated in

equatorial rift highlands is trapped first in Ugandan lakes and next in the Sudd marshes of South Sudan (Garzanti et al., 2018a). The three main detrital components have different grain size, and their mixing in different proportions along the Nile sediment-routing system explains the observed strong grain-size control on sediment composition (Fig. 2). Volcanic detritus is finer-grained, and thus markedly concentrated in silt to very-fine sand fractions carried largely as suspended load, whereas coarser basement-derived detritus increases with increasing grain size of Blue Nile and main Nile bedload sand. Upper fine to lower-medium grained quartzose eolian sand dominates the coarsest fractions of modern Nile Delta beaches and dunes (Garzanti et al., 2015).

2.3. The Nile Cone

The siliciclastic succession of the Nile Cone is estimated to have a compacted sediment volume of 581,000 km^3, with a thickness of 3.5 and 5 km reached by Oligocene and Miocene strata offshore of the Rosetta mouth and in the Damietta mouth depocenter, respectively. Plio-Pleistocene strata are more evenly distributed, with an estimated compacted volume of 188,000 km^3, and a maximum thickness of 3.5 km in the central part of the Delta (Macgregor, 2012).

Mineralogical information on the stratigraphic succession of the offshore Nile Delta is provided in Zaghloul et al. (1980) and Salem et al. (2005). Turbidites of the Nile submarine fan have been studied during DSDP Leg 13, but drilling to a depth of only 272 m did not reach beneath the Quaternary at Site 131. Quaternary turbidites of the Nile Cone range from quartz-rich feldspatho-quartzose to quartzose with K-feldspar ≥ plagioclase, a few sedimentary (shale, siltstone, limestone) and metamorphic (micaschist, gneiss, quartzite) rock fragments, and only a few basaltic rock fragments (Bartolini et al., 1975). Transparent-heavy-mineral suites are not rich and chiefly consist of hornblende, clinopyroxene and epidote, with minor amounts of zircon, garnet, staurolite, tourmaline, and rutile (Ryan et al., 1973).

3. Petrography of Nile Delta sand through time

Sixteen sand samples from subsurface Nile Delta cores, deposited by turbidity currents (Samuel et al. 2003) and mostly representing relatively coarse-grained channel-axis sediments, were selected for petrographic analysis (Fig. 1). In each thin section, prepared from a split aliquot of the bulk sample impregnated with Araldite, 400 points were counted according to the Gazzi-Dickinson method (Ingersoll et al. 1984). Sediments were classified by their main components exceeding 10%QFL (e.g., in a litho-feldspatho-quartzose sand Q > F > L > 10%QFL; Garzanti, 2016). Among lithic-poor sands, quartz-rich feldspatho-quartzose (Q/F > 4), quartzose (Q/F > 9), and pure quartzose (Q > 95%QFL) compositions were distinguished (Garzanti et al., 2018b). Median grain size was determined in thin section by ranking and visual comparison with in-house standards sieved at 0.25 ϕ sieve interval. Detrital components are listed in order of abundance throughout the article.

3.1. Modern Nile and Delta

Before closure of the Aswan High Dam, the Nile carried to the Mediterranean Sea feldspatho-quartzo-lithic volcaniclastic silt as suspended load and very-fine-grained feldspatho-litho-quartzose to fine-grained litho-feldspatho-quartzose sand as bedload (Fig. 3A). During the following decades, mixing with medium-grained quartzose and heavy-mineral-poor sand windblown from the Sahara Desert has led to a slight increase in quartz and decrease in heavy-mineral concentration (Fig. 2). Plagioclase invariably prevails over K-feldspar. Rock fragments are mostly represented by mafic volcanic grains, with subordinate intermediate or felsic volcanic, metamorphic, and sedimentary grains.

Nile Delta sands are enriched further in windblown quartz from the Sahara, especially in coarser size classes, and composition ranges from feldspatho-litho-quartzose to quartz-rich feldspatho-

quartzose in beaches and from litho-feldspatho-quartzose to quartzose in dunes (Fig. 3B, 3C). Plagioclase generally prevails slightly over K-feldspar. Mafic and subordinate intermediate or felsic volcanic rock fragments prevail over metamorphic grains (gneiss, schist, metabasite); sedimentary rock fragments are few (limestone, siltstone, chert). Biotite and subordinate muscovite are minor.

3.2. Pleistocene to Oligocene

The studied sand samples from offshore Nile Delta cores are mostly upper-fine to medium grained, median grain size ranging from 170 to 500 μm (2.6 to 1 ϕ). Only sample ND42, probably representing a levee deposit on the upper slope, is very-fine grained (~100 μm). Petrographic composition ranges from feldspatho-quartzose to quartz-rich feldspatho-quartzose in Pleistocene strata (Fig. 3D, 3E), and from quartz-rich feldspatho-quartzose to quartzose in Pliocene and Miocene strata (Fig. 3F, 3G, 3H). Oligocene sand is pure quartzose (Fig. 3I). Plagioclase invariably prevails over K-feldspar. Volcanic rock fragments, represented by frequently altered or glauconized grains, are most abundant in Plio-Pleistocene samples, where they commonly display microlitic and lathwork texture. Felsitic volcanic lithics occur throughout the section. A few granitoid rock fragments and micas occur, along with minor sedimentary (shale, siltstone/sandstone, limestone, dolostone) and metamorphic grains (quartz-mica, epidosite, porphyroid, chlorite schist). The very-fine-grained Pleistocene sample ND42 is the richest in plagioclase, volcanic rock fragments, and heavy minerals (Fig. 4).

3.3. Comparison with modern sands and stratigraphic trends

The very-fine-grained Pleistocene sample ND42 has a petrographic composition close to both average beach and finer-grained dune sand in the modern Delta, whereas the medium-grained

Pleistocene sample ND41 is as quartz-rich as coarser dune sand (Fig. 4). The other upper-fine to lower-medium Plio-Pleistocene sand samples contain significant amounts of feldspars and volcanic rock fragments, whereas quartz increases at the expense of the other detrital components in upper-medium sand. Detrital modes of Plio-Pleistocene samples and of modern beaches and dunes are therefore comparable. The slightly higher quartz content and lower heavy-mineral concentration of the former is explained at least in part by the coarser grain size of the analyzed cored samples, suggesting greater contribution of relatively coarse Saharan sand. Quartz increases and heavy-mineral concentration decreases further in Miocene samples, and even further in Oligocene samples, which are much richer in quartz than modern Delta sand although they still contain volcanic detritus (Table 1).

4. Heavy minerals in Nile Delta sand, silt, and mud through time

All sixteen sand samples analyzed for framework petrography were analyzed for heavy minerals. Additionally, we have analyzed twelve samples of mud and eight samples of silty sand or sandy silt from Oligocene to Pleistocene strata. A split aliquot of each sample was wet sieved using standard sieves in steel and hand-made tissue-net sieves (15 μm mesh). For practical reasons and to obtain a faithful characterization of heavy minerals minimizing the loss of those contained in the tails of the size distribution (Garzanti et al., 2009), we chose to analyze 4 ϕ-wide size-windows for sand (32-500 μm) and sandy silt (15-250 μm), and the 15-63 μm size-window for mud. Heavy minerals were separated by centrifuging in sodium metatungstate (density ~2.90 g/cm^3), and recovered after partial freezing of the test tube with liquid nitrogen. The heavy fraction *H* thus obtained was weighed, split carefully with a micro-riffle box, and mounted on a glass slide with Canada balsam for counting. Between 200 and 300 transparent heavy minerals were counted by the "area method" in most samples. Rock fragments, iron-rich soil clasts, phyllosilicates (chlorite, biotite, hydro-biotite), carbonates, and minerals of suspect authigenic or anthropogenic origin

(e.g., Fe-oxides, Ti-oxide aggregates, barite) were not considered as an integral part of the transparent-heavy-mineral suite. In samples dominated by such altered or spurious grains, we counted all transparent-heavy-mineral grains present in the slide (Fleet method; Galehouse, 1971). Grains of uncertain identification were checked with Raman spectroscopy (Ando and Garzanti, 2014). For each heavy-mineral species, the percentage of corroded, etched, deeply etched, and skeletal grains was recorded (Andò et al., 2012). Transparent-heavy-mineral suites are described as "extremely poor" (tHMC < 0.1), "very poor" (0.1 ≤ tHMC < 0.5), "poor" (0.5 ≤ tHMC < 1), "moderately poor" (1 ≤ tHMC < 2), "moderately rich" (2 ≤ tHMC < 5), "rich" (5 ≤ tHMC < 10), and "very rich" (10 ≤ tHMC < 20). The transparent-heavy-mineral concentration (tHMC) index is the volume percentage of transparent heavy minerals in the sample. The ratio between the transparent-heavy-mineral fraction and the total weight of the heavy fraction (tHM/H%) is newly defined formally here as a simple additional parameter helpful to detect intrastratal dissolution. The Source Rock Density (SRD) index is the weighted average density of extrabasinal terrigenous grains (Garzanti and Andò, 2007a). The sum of zircon, tourmaline and rutile over total transparent heavy minerals is classically used to estimate the “durability” of the assemblage (ZTR index of Hubert, 1962).

4.1. Modern Nile and Delta

Before closure of the Aswan High Dam, fluvial sediments reaching the Delta contained rich to very rich transparent-heavy-mineral suites dominated by augitic clinopyroxene with subordinate amphibole and epidote, and very minor garnet, olivine, titanite, and apatite. Modern beach and dune sands of the Delta contain mostly rich clinopyroxene-amphibole-epidote suites with minor garnet, zircon, titanite, staurolite, tourmaline, rutile, apatite, and rare kyanite, sillimanite, andalusite, pumpellyite, monazite, olivine, and Cr-spinel (Table 2). In modern sediments, transparent heavy minerals represent 76 ± 5% of the total heavy fraction *H*.

4.2. Pleistocene to Oligocene

Lower Pleistocene sediments contain moderately poor to rich amphibole-epidote suites with apatite and garnet. Sand yields more zircon and rare clinopyroxene. Transparent heavy minerals represent 53 ± 4% of the total heavy fraction.

Pliocene mud contains poor to moderately rich, epidote-dominated suites with amphibole, apatite, titanite, tourmaline, zircon, and rutile. Sandy silt yield either a moderately poor epidote-dominated suite with amphibole and apatite, or a very poor ZTR-dominated suite with epidote, apatite, garnet, and minor Cr-spinel. Sand yield either a moderately poor epidote-amphibole suite, or a very poor epidote-rich suite with zircon, garnet, rutile, titanite, apatite, tourmaline, staurolite, kyanite, and amphibole. Transparent heavy minerals represent 46 ± 16% of the total heavy fraction in sand samples, and 25 ± 1% in sandy silt and mud samples.

Miocene mud, sandy silt, and sand contain very poor to extremely poor, ZTR-dominated assemblages with apatite. Sand yields more garnet and locally rare clinopyroxene. Titanite, monazite, and Cr-spinel are minor. Transparent heavy minerals represent 21 ± 5% of the total heavy fraction in sand samples, and only 5 ± 3% in sandy silt and mud samples.

Oligocene mud, sandy silt and sand contain very poor to extremely poor, ZTR-dominated assemblages (Table 2). Apatite is more common and chloritoid found sporadically in muds. A few epidote and kyanite grains were found in sandy silts. Monazite and Cr-spinel are minor. Transparent heavy minerals represent 41 ± 12% of the total heavy fraction in sand samples, and 5 ± 2 % in sandy silt and mud samples.

4.3. Comparison with modern sediments and stratigraphic trends

At a cursory look, heavy-mineral suites in the cored Cenozoic succession bear little in common with those in modern Nile and Delta sands. Modern sediments are invariably dominated by clinopyroxene derived from the Ethiopian continental flood basalts, whereas only one lower Pleistocene sand and one Miocene sand yielded rare pyroxene grains. On closer inspection, however, all transparent-heavy-mineral species display clear unidirectional stratigraphic trends (Table 2). Relative to modern sediments, transparent-heavy-mineral concentration is reduced to a half or a third in lower Pleistocene strata, becomes almost one-order-of-magnitude less in upper Pliocene strata, and almost two-orders-of-magnitude less in Oligo-Miocene strata. Transparent heavy minerals represent three-fourths and half of the heavy fraction in modern and Pleistocene sediments, respectively, but less than 10% in Oligo-Miocene sandy silt and mud. Amphibole increases in relative frequency in the lower Pleistocene, it is common only locally in the Pliocene, and it is virtually absent in the Miocene and Oligocene. Epidote increases markedly in lower Pleistocene sediments, reaches a maximum in Pliocene mud, and then decreases sharply in Oligo-Miocene strata, where it is only sporadically present. Similar trends are displayed by garnet, titanite, and staurolite, which are uncommon in modern sand, become relatively more abundant with depth, reach their maximum in Pliocene (titanite, staurolite) or Miocene samples (garnet), and finally decrease and become sporadic in Oligocene strata. Apatite reaches a maximum in lower Miocene mud and is still common in Oligocene sediments. Chrome spinel, negligible in modern sand, becomes progressively more significant with stratigraphic age and burial depth. Monazite follows a similar trend. Zircon, tourmaline and rutile, invariably minor in modern sand, are locally common in Pliocene sand and silty sand, consistently dominant in Miocene sediments, and overwhelming in Oligocene sand.

5. Provenance or diagenesis?

Petrographic and heavy-mineral trends observed throughout the Cenozoic Nile Delta succession define five compositionally distinct chronostratigraphic intervals: modern (sampled both before and after closure of the Aswan High Dam), lower Pleistocene, Pliocene, Miocene, and Oligocene (Fig. 4). In principle, the marked compositional differences observed may be ascribed to multiple and potentially interacting autocyclic and allocyclic factors, including changes in tectonic activity, climate changes controlling water and sediment fluxes as well as pathways and intensity of eolian sediment transport, paleodrainage changes and river captures, grain-size control, hydraulic sorting, and selective breakdown of nondurable grains by mechanical or chemical processes before final deposition. But the key question is whether these signatures are chiefly primary (i.e., originally present at the instant of deposition) or secondary (i.e., produced by the progressive dissolution of unstable detrital components during burial diagenesis). In the former case, they carry information that can be read directly in terms of lithology, location of source areas, and changing tectonic, magmatic, or climatic regimes in the catchment; but not necessarily so in the latter case. This is the tangle invariably involved with the interpretation of detrital modes in ancient sandstones.

5.1. What does sediment composition tell us?

The petrographic composition of cored Pleistocene sand is not much different from that of modern Nile Delta beaches and dunes of similar grain size, or of Quaternary turbidites of the Nile submarine fan (Bartolini et al., 1975). Heavy-mineral suites, however, are markedly different, principally because they lack pyroxene in stark contrast with clinopyroxene-dominated suites of modern Nile sediments. In Quaternary turbidites, clinopyroxene is common but less abundant than amphibole, and epidote increases notably with increasing burial depth (Ryan et al., 1973). In the studied Nile Delta succession, compositional differences become increasingly stronger with age and burial depth. Quartz increases progressively at the expense of feldspars and especially of mafic volcanic rock fragments (Table 1). Transparent-heavy-mineral concentration decreases

progressively, and durable minerals increase their relative abundance whereas less stable minerals decrease and eventually disappear (Fig. 5). Few clinopyroxene grains and no olivine were recorded in lower Pleistocene sediments. Amphibole decreases markedly in Pliocene strata and virtually disappears in Miocene strata, where epidote decreases drastically together with titanite, staurolite, and opaque Fe-Ti-Cr oxides. Instead, zircon, tourmaline, rutile, apatite, Cr-spinel, and monazite increase their relative frequency. Garnet and apatite decrease in Oligocene strata, where zircon reaches its maximum frequency (Table 2). In Oligo-Miocene samples, the heavy fraction becomes dominated by turbid grains, chlorite, and Ti oxides (tHM/H% < 10 in sandy silt and mud), testifying to a strong increase in post-depositional alteration.

5.2. The meaning of compositional change

Stratigraphy is essentially the art of exploring geological time. Documented in any stratigraphic layer is the ultimate result of multiple physical and chemical processes continuously changing in relative intensity through millions and millions of years across the generally vast source areas and within the depositional basin. Moreover, the effect of chemical transformations during post-depositional burial, also taking place through millions and millions of years, is invariably superposed. Although the tangle is hard to tackle, because the information at hand is invariably scarce and uncertain, we may start from the consideration that different controlling processes have a different character, and therefore leave a different mark through the stratigraphic record (Ager, 1981; Gould, 1987 p.10-16). Climatic changes are reversible, and will thus be revealed by a periodic or aperiodic, symmetric or asymmetric cyclic signal, as seen for instance in complete oxygen or carbon isotope records. Instead, tectonic or magmatic processes lead to pulsed geological events that will be documented by a series of single irreversible changes. Intrastratal dissolution, also an irreversible but progressive chemical process, will leave a systematic unidirectional trace throughout the stratigraphic succession. Finally, hydraulic-sorting processes

act locally and erratically, and principally affect ratios between detrital minerals differing markedly in size, density, or shape (Komar, 2007).

In the Nile Delta stratigraphic record, we do see irregular mineralogical changes at the small scale, suggesting superposition of multiple controls, but the long-term general picture is that of steady mineralogical trends. Such a progressive compositional evolution, poorly compatible with the mark of either punctuated paleotectonic/paleogeographic episodes or cyclic factors, does not indicate a reversible process such as climate forcing, but rather the control of an irreversible process such as intrastratal dissolution, operating on the background of a relatively stable paleotectonic scenario.

All of the analyzed samples down to the Oligocene contain some volcanic rock fragments, and Cr-spinel notably increases its low relative abundance with age and burial depth, testifying to the presence of detritus from mafic rocks since the lower Oligocene. These clues concord with multi-technique geochemical and geochronological data indicating that the Nile has maintained its Ethiopian connection since the early Oligocene (Fielding et al. 2018). We conclude that inter-sample compositional variability of Cenozoic Nile Delta sediments is principally controlled by post-depositional chemical processes, and that the five compositionally distinct rock-time intervals identified do not represent provenance petrofacies (*sensu* Dickinson and Rich, 1972) but rather "diagenetic minerofacies" (an expression newly introduced here to designate a standard mineralogical assemblage largely controlled by selective diagenetic dissolution).

6. Detangling the tangle

Based on a rough statistical analysis of compositional parameters, displaying a steady exponential decay with burial depth for less durable components (coefficients of determination R^2 = 0.52 and 0.66 for feldspars and volcanic rock fragments, R^2 = 0.80 and 0.84 for transparent-heavy-mineral concentration and ferromagnesian minerals) and a sharp linear increase of the ZTR index (R^2 =

0.95), we evaluate that at least half to two-thirds of the variability in petrographic modes and between four-fifths and 95% of transparent-heavy-mineral suites observed in Nile Delta cores is accounted for by selective diagenetic dissolution (Fig. 6).

6.1. Detecting grain-size control and mixing with eolian sand

Inter-sample variability is not observed uniquely among sample groups of different age and burial depth but also within each sample group. Starting from lower Pleistocene strata, which underwent less intense diagenetic dissolution, we note a marked difference in composition between very-fine sand sample ND42 (Q/L 9) and medium sand sample ND41 (Q/L > 100). Such a sharp increase in the quartz/lithic ratio with grain size may have been partly caused by selective post-depositional leaching in coarser and thus more porous and permeable layers, but it is likely to be an original primary signature as well. The same grain-size control is observed in fact in both modern Nile River and Nile Delta sediments, where the volcaniclastic Ethiopian component is enriched in finer size fractions and eolian quartz progressively in coarser sand fractions (figs. 26 to 33 in Garzanti et al., 2015). Inspection of Fig. 4 shows that Pliocene samples also display a compositional difference between fine to lower-medium sand samples (Q/L 10-18) and upper-medium sand samples (Q/L 33-63). This difference may be retained even in Oligocene strata, where lithic fragments are slightly more common in fine sand sample ND40 (Q/L 50) than in medium sand sample ND32 (Q/L 69).

Eolian dunes in the Egyptian Sahara mostly consist of durable minerals (Q/QFL% 96 ± 1 and ZTR 42 ± 5 in the Western Desert), which makes it hard to isolate the effect of eolian mixing from that of intrastratal dissolution in our core samples. If environmental control had been a major cause of inter-sample mineralogical variability, however, then we would expect to see compositional cycles, perhaps with humid stages characterized by more varied mineralogical suites of Nile

provenance alternating with dry stages characterized by dominant quartz and durable heavy minerals of Sahara provenance. This we do not see.

6.2. Checking for hydraulic-sorting effects

Hydraulic-sorting effects are difficult to quantify in diagenized ancient sandstones. One way is to calculate ratios between minerals characterized by different density and similar resistance to dissolution (e.g., zircon Z, rutile R, monazite M, or Cr-spinel S *versus* tourmaline T, and garnet G *versus* apatite A). In the modern Delta, the average Z/T, R/T, M/T, S/T, and G/A ratios are estimated to be 1.3, 0.4, 0.1, ~0, and 3.4 in beach and dune sand not markedly affected by hydraulic-sorting effects, rising respectively to 26, 6, 1, 0.02, and 19 in the Rosetta magnetite placer (Garzanti et al., 2015). Similar resistance to dissolution of each mineral couple defined above is confirmed by the poor correlation between any of these ratios and core depth. In core samples, the average Z/T and G/A ratios are higher in sand, and the R/T ratio in sand and sandy silt. None of the analyzed mud, sandy silt, and silty sand samples shows anomalously high values, whereas four sand samples (ND1, ND11, ND18, and ND 32) show systematically high ratios (Z/T between 4 and 9, R/T between 2 and 4, M/T between 0.1 and 0.5, S/T up to 0.17, and G/A up to 4). These samples, therefore, do display an anomalous concentration of densest minerals, which is ascribed to selective removal of slow-settling grains by contouritic bottom currents in offshore deep-water environments (Stow and Lovell, 1979).

6.3. Extracting provenance information

There have been many diverse reconstructions of Cenozoic drainage evolution in northeastern Africa (McCauley et al., 1986; Burke and Wells, 1989; Said, 1993; Goudie, 2005; Macgregor, 2012). The reason why such a variety of contrasting scenarios has been envisaged is that clues are

scarce and invariably circumstantial. Detrital mineralogy, one of the theoretically best tools at our disposal, is made blunt by the diagenetic loss of key provenance tracers such as olivine or pyroxene. Only in modern settings can we expect that sediment composition faithfully reflects what is happening in the source areas and along the sediment-routing system (i.e., provenance plus "environmental bias"). In ancient sedimentary rocks, mineralogical changes caused by intrastratal processes ("diagenetic bias") will be invariably superposed to different degrees onto the original detrital signals. If we do not cautiously attend the thorny task of unraveling first the post-depositional modifications undergone by mineralogical assemblages in order to extract the generally faint primary signals from the generally loud secondary noise, then we are prone to incur gross mistakes in our provenance diagnoses.

The Nile Delta succession presents an exemplary case clearly illustrating such a risk, because modern sediments contain abundant labile ferromagnesian minerals that may dissolve rapidly at depths of a few tens of meters only. Bowman (1931 p.260) noted a drastic decrease in the abundance of clinopyroxene in ancient Nile sediments near Cairo already at depths between 18 and 47 m. Sandford and Arkell (1939 p.71-75) described Pliocene sediments as quartz sands lacking hornblende. A decade later, Shukri (1950 p.523-528) furthered these observations on Pliocene and Plio-Pleistocene sediments, but failure to realize the overwhelming effect of diagenetic dissolution led him to conclude that the Blue Nile and Atbara tributaries sourced in Ethiopian volcanic highlands connected with the Nile catchment only in very recent prehistoric ("*Middle Palaeolithic*") times. This has remained ever since one of the major arguments that led authors to disbelieve that an Ethiopian connection could have existed before recent and even very recent times (Nachmias, 1969; Zaghloul et al., 1980; El Sisi et al., 1996; Issawi and Osman, 2008; Macgregor, 2012; Leila et al., 2018). But if instead of an unstable tracer of mafic provenance such as pyroxene we look at the stratigraphic distribution of a durable mineral such as Cr-spinel, then we observe that its relative concentration increases notably with age and burial depth, and that its absolute concentration is between 1 and 10 ppm in Oligo-Miocene sand and mud. Moreover,

volcanic rock fragments are common in upper Miocene sandstones of the onshore Nile Delta subsurface, where they are largely replaced by chlorite (Salem et al., 2005). Identifiable basaltic grains are rare in our Oligo-Miocene samples, but felsic volcanic rock fragments, which are chemically more durable, occur in virtually unchanged proportions throughout the section. Provenance tracers least affected by diagenesis, such as U-Pb age spectra of detrital zircons or Nd isotope compositions, indicate relatively constant provenance and paleodrainage over time (Fielding et al., 2018).

6.4. Looking for climate change

Extracting information on changing paleoclimate from mineralogical suites of strongly diagenized sedimentary successions is even more difficult than to retrieve provenance information. Both pre-depositional "*in situ*" weathering and post-depositional intrastratal dissolution are chemical processes, and both tend to eliminate unstable minerals selectively by acid hydrolysis (Milliken, 2003). The effect, however, may differ, because geochemical environments may be markedly different. Garnet and apatite, for instance, typically prove to be very labile during pedogenetic alteration but resistant during diagenesis (Velbel, 1993; Morton et al., 2012). This offers us the possibility to use ratios between mineral couples with similar density, shape, and chemical durability such as apatite and tourmaline (ATi index of Morton and Hallsworth, 1999), which are expected to respond similarly to hydrodynamic and diagenetic processes but differently to weathering in even mildly acidic soils (van Loon and Mange, 2007). In the Nile Delta succession, the ATi index tends to decrease with age in all size fractions, and shows the highest values in the Pleistocene and the lowest values in the Oligocene. But it is hard to say whether this may be a primary paleoclimate signal or simply reflects a greater stability of tourmaline relative to apatite during deep burial diagenesis.

Today, weathering effects are minor for Nile sediments carried across hyperarid Saharan lowlands to the Mediterranean Sea. Chemical leaching is intense only in the hot-humid equatorial part of the Nile catchment (Garzanti et al., 2013a, 2013b). Erosion in Ethiopian highlands is fast, and only sediments carried by the left-bank southern tributaries of the Blue Nile are moderately weathered (Garzanti et al., 2015). In the past, climate changed repeatedly in northern Africa (Griffin, 2002), and there is strong evidence of wetter climate in the Sahara before 5 ka (Box et al., 2011; Woodward et al., 2015). However, it is hard to believe that weathering could have been strong enough to transform feldspatho-litho-quartzose volcaniclastic sediments into a quartz-rich residue. Strong pre-depositional chemical weathering is ruled out by common and ubiquitous apatite, which is highly unstable in tropical soil profiles particularly in the presence of humic acids (Bateman and Catt, 2007; Van Loon and Mange, 2007; Morton et al., 2012).

During the late Quaternary, climate change associated with repeated northward or southward shifts of the inter-tropical convergence zone have influenced markedly sediment fluxes from subequatorial Africa, induced drastic fluctuations in Nile hydrology, and reduced deep-water circulation in the Mediterranean Sea (Williams et al., 2015). Such climatic fluctuations must have affected mixing proportions between volcanic and metamorphic detritus carried by the Nile from Ethiopian highlands with largely windblown quartz-rich sand derived locally from the Western Desert. The water flux that allows the river to cross the Sahara is fuelled by equatorial rains collected largely in Lake Victoria, and from there conveyed along the White Nile (Sutcliffe and Parks, 1999). Lake Victoria began to overflow to the north only around 400 ka, but it became disconnected with the White Nile repeatedly during subsequent periods of aridity, the most recent of which was roughly coeval with the Last Glacial Maximum. During dry periods, Nile waters were unable to flow permanently across the Sahara, and the lower course was invaded locally by sand dunes and transformed into a series of lakes only temporarily connected (Vermeersch and Van Neer, 2015). The modern hydrological regime of the Nile is only as old as 14.5 ka, when overflow from Lake Victoria was re-established by strengthening of the summer monsoon

(Williams and Talbot, 2009). Climatic changes are therefore likely to have regulated short-term changes in quartz abundance in Nile Delta sediments through time. These changes might account for about one-third of compositional variability, but a precise evaluation is prevented by the masking effect of overwhelming diagenetic control.

7. Diagenetic control on heavy-mineral suites

In the Nile Delta, geothermal gradients range from 18.1 to 26.5°C/km, somewhat lower than those generally observed away from tectonic plate boundaries (i.e., 100°C are reached at depths between 3 and 4.5 km; Riad et al., 1989). The presence of upper-fine to medium-grained sand layers ensures good permeability and fluid circulation throughout the succession.

7.1. Differential dissolution in mud, silt, and sand

Inspection of Table 2 indicates that, apart from some minor differences discussed below, mud, sandy silt, and sand samples do not contain markedly different transparent-heavy-mineral assemblages in terms of both concentration and spectrum. This observation challenges the long-held view (e.g., Blatt and Sutherland, 1969) that intrastratal dissolution is strongly controlled by grain size and permeability, and that consequently it should be far more extensive in porous sand than in much less permeable mudrock. Rather, within the offshore Nile Delta succession the percentage of transparent heavy minerals on the total heavy fraction (tHM/H% index) decreases more rapidly with depth in mud samples than in sand samples (Table 2).

The lower Pleistocene sample ND42 - the finest grained of all analyzed sands - is the one containing most heavy minerals and mafic volcanic rock fragments, but negligible clinopyroxene (Fig. 3D). Diagenetic dissolution of pyroxene, therefore, was not less extensive than in the much coarser-grained lower Pleistocene sample ND41, which yielded instead a few etched

clinopyroxene grains. A plausible reason why the finer-grained sample ND42 contains more volcanic rock fragments is grain-size control. As observed in the modern Delta, finer-grained sand has larger proportions of Nile-derived volcanic detritus and heavy minerals, whereas coarser-grained sand has larger proportions of quartzose Saharan sand (fig. 26 in Garzanti et al., 2015). Grain-size control may explain why garnet and staurolite, relatively common in coarser-grained Saharan dunes and minor in finer-grained Nile sediments, are more abundant in Pliocene and Miocene Delta sands than in muds. More abundant epidote in Pliocene mud than in coeval sand may be an effect of suspension sorting (*sensu* Slingerland, 1984), because epidote has been observed to concentrate in the silt fraction in other large fluvial and turbiditic systems (Garzanti et al., 2011; Limonta et al., 2015). The greater abundance of denser heavy minerals (zircon, monazite, garnet, staurolite) in sand samples, and of less dense heavy minerals (apatite, tourmaline) in mud samples within each stratigraphic interval (Table 2) is also ascribed to suspension-sorting rather than to differential preservation in layers with different permeability. The widely held, plausible idea that (Morton and Hallsworth, 2007 p.237): "*siltstones and mudstones also have poor porosity and permeability, and thus tend to preserve more diverse heavy-mineral assemblages than adjacent sandstones (Blatt and Sutherland, 1966)*" is thus largely contradicted by observations in this Nile Delta case study. Alteration of unstable minerals hosted in sandstone and shale in comparable degrees is documented also in the classical Cenozoic succession of the Gulf of Mexico (Milliken, 1992).

Because sand, silt, and mud samples do not display notably different transparent-heavy-mineral assemblages within each stratigraphic interval (Table 2), they will be considered together in the following discussion.

7.2. Relative mineral durabilities

If a paleo-Nile River with Ethiopian connection has existed since the Oligocene, and if detrital assemblages supplied to the Delta have consequently remained broadly constant throughout the studied succession, then those minerals progressively enriched down-core are those that better endured intrastratal dissolution. Under this assumption, a sequence of relative mineralogical durabilities in the diagenetic environment can be established (Fig. 7). Among transparent heavy minerals, olivine is not found and clinopyroxene is rare at burial depths of 1200 m, and amphibole and staurolite virtually disappear below 2500 m. Instead, zircon, tourmaline, apatite, monazite, and Cr-spinel increase their relative proportions at greater depths. Inspection of the heavy-mineral distribution chart in Table 2 suggests the following sequence of chemical durability during burial (the position of minerals between brackets, which are rare in the studied samples, is only indicative): zircon > rutile ≥ tourmaline, (Cr-spinel) ≥ apatite ≥ monazite, (chloritoid) > garnet, (kyanite) > titanite > staurolite > epidote > amphibole > clinopyroxene > olivine. Among main framework grains: quartz > felsic volcanic rock fragments > feldspars > mafic volcanic rock fragments. Quartz resulted to be as durable as zircon, tourmaline, or rutile. Rather surprisingly, K-feldspar appeared to be not less labile than plagioclase (Table 1).

7.3. Quantifying heavy-mineral loss

The observed sequence of mineral durabilities to chemical dissolution during burial is similar to those reported from stratigraphic sections worldwide (e.g., Milliken, 2007; Morton and Hallsworth, 2007). The hypothesis that all studied sediments are Nile-derived, therefore, is certainly not falsified (*sensu* Popper, 1959). Under this assumption, by using the composition of modern Delta sediments as a reference, we may tentatively quantify how much of the original detrital assemblage has been dissolved in sand and mud at diverse burial depths. Our calculations indicatively suggest that transparent heavy minerals do not represent more than 20% of the original assemblage in sediments buried less than ~ 1.5 km, more than 5% in sediments buried

between 1.5 and 2.5 km, and more than 1% for sediments buried more than 4.5 km. These impressive figures confirm the view that "*the importance of post-depositional dissolution cannot be overemphasized*" (Mange and Maurer, 1992).

8. Diagenetic minerofacies as a working tool

This Nile case illustrates well the difficulties involved in the assessment of mineralogical changes operated by post-depositional dissolution and the complexities faced while unraveling primary provenance signals from secondary diagenetic transformations in ancient siliciclastic rocks. The provenance interpretation of Cenozoic successions is already a theatre of ambiguities, and most Mesozoic cases present conundrums hard to tackle (e.g., Wang et al., 2016). If the system remains sealed for long from circulating pore fluids thus preventing dissolution reactions to proceed, however, even Paleozoic strata may preserve a wide spectrum of detrital species including ferromagnesian minerals (e.g., Cawood, 1983; Morton et al., 2011).

As an example of ambiguous evidence, the typical sequence in which marker minerals appear upsection in Neogene Himalayan foreland-basin successions (ZTR -> garnet -> staurolite -> kyanite -> sillimanite; Szulc et al., 2006; Vögeli et al., 2018) may reflect the unroofing of progressively higher-grade metamorphic source rocks with time as well as the progressive dissolution of less durable minerals with increasing age and burial depth. Making a reliable provenance diagnosis proves to be exceedingly difficult wherever small differences in detrital signatures among similar potential sources are blurred by diagenetic bias, as in the case of Neogene turbidites derived from the eastern Himalaya (Limonta et al., 2017). In more fortunate cases - where the geological framework is well constrained, end-member mineralogical signatures can be defined precisely based on the study of modern sands, and detrital modes are diagnostic of one dominant source area - accurate quantitative provenance assessments can still be made, and even the amount and type of detrital minerals lost by chemical dissolution during diagenesis

tentatively reckoned, as in the classical case of the Apenninic foredeep (Gazzi, 1965; fig. 4 in Garzanti and Malusà, 2008). The chemical reactivity of detrital minerals, however, depends not only on pore-fluid temperature - which may vary widely at a given depth because of markedly different geothermal gradients - but also on pore-fluid composition, and the relationships between dissolution rates and burial depth may thus differ notably from basin to basin.

Heavy-mineral suites generated in orogenic and anorogenic plate-tectonic settings are expected to differ significantly (Nechaev and Isphording, 1993; Garzanti and Andò, 2007b). Nevertheless, the detrital signatures of ancient orogenic clastic wedges bear much in common with those of offshore Nile Delta sediments generated entirely along a nascent divergent plate-margin. Such mineralogical similarities are highlighted by a comparison between Cenozoic successions deposited at the outlet of two major fluvial systems in opposite geodynamic scenarios, the Nile and the Ganga-Brahmaputra draining the Himalayan collided range (Fig. 8).

8.1. The Bay of Bengal case

The Bengal fluvial, deltaic, and turbiditic system - where detritus has been dominantly supplied by erosion of the Himalayan range throughout the Neogene (France-Lanord et al., 1993; Najman et al., 2008) – is one case in which the effect of diagenesis on detrital modes was investigated extensively both in outcrop and in the subsurface (Morton and Hallsworth, 2007 p.224-225; Andò et al., 2012; Najman et al., 2012). Modern Ganga-Brahmaputra sediments are litho-feldspatho-quartzose metamorphiclastic with rich amphibole-epidote-garnet suites (tHMC 6 ± 2, ZTR 5 ± 2; Garzanti et al., 2010, 2011). In the subsurface succession, heavy-mineral assemblages show progressive systematic changes with burial depth. Below 0.5 km, pyroxene disappears and sillimanite becomes rare. Between 1 and 2 km, amphibole decreases rapidly, and consequently assemblages are relatively enriched in garnet and epidote. Between 2 and 3 km, amphibole and sillimanite disappear, epidote progressively decreases, and assemblages are relatively enriched

further in garnet (HMC < 1, ZTR 10 ± 5). Between 3 and 4 km, kyanite and titanite first, staurolite next, and finally chloritoid decrease and tend to disappear, leaving a very poor, garnet-dominated heavy-mineral residue including zircon, tourmaline, rutile, apatite, and Cr-spinel (HMC < 0.5, ZTR 15 ± 5).

8.2. Vertical trends in contrasting settings

Classical heavy-mineral studies from the Gulf of Mexico (Bornhauser, 1940; Cogen, 1940; Milliken, 1988), North Sea, and Bengal basin (Morton and Hallsworth, 2007) have shown that the burial depth at which each non-durable mineral starts to dissolve and is finally leached out may differ widely. All minerals, for instance, are preserved to much greater depths in the Gulf of Mexico, where low geothermal gradients prevail (20-30°C/km; Sharp et al., 1988), than in the North Sea, where gradients are similarly low in correspondence with structural highs but notably higher for all major basins (30-40°C/km; Evans and Coleman, 1974). However, least durable (e.g., olivine, pyroxene, amphibole), moderately durable (epidote, titanite, kyanite, staurolite, garnet), and most durable minerals (zircon, tourmaline, rutile, apatite, Cr spinel, monazite) display a remarkably similar relative behavior. This justifies the definition of a standard vertical sequence of mineral facies ("minerofacies"), which will serve in the first place as a reference to detect diagenetic control in ancient sedimentary successions. In the second place, looking for the inevitable discrepancies among different basins will help us to retrieve relevant information about: a) provenance (e.g., greater abundance of garnet in orogenic settings or presence of Cr-spinel revealing mafic/ultramafic sources); b) climatic conditions (e.g., unexpected absence of apatite suggesting acid pedochemical weathering); c) environmental processes (e.g., anomalous ratios between ultradense and equally resistant low-density minerals revealing hydraulic sorting); d) geothermal gradient and composition of intrastratal fluids. Provenance, climatic, or environmental information, however, will be safely retrieved only from those stratigraphic successions that

display mineralogical trends in contrast with the expected stratigraphic sequence of diagenetic minerofacies (i.e., unstable minerals increasing with age), whereas utmost care should be taken in the much more common opposite case.

8.3. Diagenetic minerofacies in outcrops and cores

As a first step toward the definition of a standard sequence of diagenetic minerofacies, Garzanti and Andò (2007a p.535-538) observed the following broad correspondence between heavy-mineral concentration and the relative abundance of diverse heavy-mineral species in ancient foreland-basin and remnant-ocean-basin sandstones derived from the Alpine-Himalayan orogen: *zone a*) moderately-poor garnet-epidote suite with rare amphibole (ZTR 10 ± 5); *zone b*) poor garnet-dominated suite with subordinate epidote (ZTR 25 ± 15); *zone c*) very poor suite including garnet and locally Cr-spinel (ZTR 50 ± 20); and, *zone d*) extremely poor suite dominated by the most durable minerals (ZTR 90 ± 15). The systematic vertical superposition of *zones d*, *c*, *b*, and *a* observed from the bottom to the top of an exposed sedimentary succession points to a strong diagenetic overprint of the original provenance signature.

Relative to field outcrops, the study of cores through a thick sedimentary succession deposited at the mouth of a large river has several advantages: 1) the record is continuous; 2) burial depth is known; 3) maximum temperature is generally known; and, especially 4) under the assumption that paleodrainage has not changed significantly, the detrital assemblage at the instant of deposition can be considered as broadly constant through time. This is the reason why the offshore Nile Delta and Bay of Bengal cases, integrated by observations on other well studied sedimentary basins worldwide, offer a suitable basis to define a standard sequence of diagenetically-controlled heavy-mineral zones, which we call here “minerofacies” (Table 3). Because the burial depth to which each mineral species is preserved depends on its original abundance, on the geothermal gradient, and on pore-fluid composition - and thus varies significantly from basin to basin - the vertical

zonation described below is indicative only, the focus being on the progressive decrease in transparent-heavy-mineral concentration with burial depth rather than on mineralogical ratios, which may vary significantly from case to case. Moreover, this issue may be complicated by the authigenic growth of minerals at high diagenetic temperatures (e.g., Fe-rich epidote at ≥ 200°C), a possible occurrence that is not contemplated here.

8.4. A standard sequence of diagenetic minerofacies

Minerofacies 0

modern sediments (indicatively Q/QFL% 65 ± 20, tHMC 4 ± 2, SRD 2.70 ± 0.02, tHM/H% 60 - 90, ZTR 2 ± 2). Detrital assemblages in modern sediments generated in orogenic and anorogenic settings differ very markedly. Ganga-Brahmaputra sediments are much richer in metamorphic detritus (high-rank metamorphic rock fragments, micas, garnet, chloritoid, staurolite, kyanite, and sillimanite) and subordinately in sedimentary detritus (sedimentary rock fragments, recycled zircon, tourmaline, and rutile). Nile sediments are much richer in volcanic detritus (mafic volcanic rock fragments, plagioclase and clinopyroxene, with minor olivine and Cr spinel). Other compositional parameters (quartz, total feldspars, heavy-mineral concentration) are broadly similar.

Minerofacies 1

very shallow burial (*hornblende zone*; indicatively Q/QFL% 70 ± 20, tHMC 2 ± 1, SRD 2.69 ± 0.02, tHM/H% 50 - 70, ZTR 5 ± 2). The least durable minerals are lost progressively with increasing burial depth. Olivine and pyroxene, even where originally abundant, may be leached out already within the first several tens of meters of burial, as observed in the Nile Delta succession. All of the more resistant minerals may consequently show a relative increase in abundance. These generally include amphibole, although hornblende gets corroded and may be severely depleted as observed in Chinese Loess deposits buried less than 200 m (Nie et al., 2013).

Minerofacies 2

shallow burial (*epidote-hornblende* zone; indicatively Q/QFL% 75 ± 20; tHMC 1 ± 1, SRD 2.68 ± 0.02, tHM/H% 40 - 60, ZTR 20 ± 10). Transparent heavy minerals, representing about half of the heavy fraction, are generally dominated by hornblende and epidote in both orogenic and anorogenic sediments. Epidote increases in relative abundance while hornblende and other unstable minerals begin to be rapidly dissolved. Garnet relatively increases much more markedly in orogenic sediments, together with relatively stable minerals such as titanite, kyanite, or staurolite. These trends, as well as the final disappearance of hornblende, are generally observed within the first (North Sea: fig. 2 in Morton and Hallsworth, 2007) or second km of burial depth (Gulf of Mexico: fig. 2 in Milliken, 2007; Bay of Bengal: fig. 13 in Andò et al., 2012; Nicobar Fan: Limonta et al., 2018; Nile Delta).

Minerofacies

moderate burial (*garnet-epidote zone*; indicatively Q/QFL% 75 ± 15; tHMC 0.5 ± 0.5, SRD 2.67 ± 0.02, tHM/H% 30 - 50, ZTR 30 ± 10). Garnet and epidote are the most abundant transparent heavy minerals in orogenic and anorogenic sediments, respectively. Garnet progressively increases with depth relatively to epidote, because the latter dissolves more rapidly. These trends, as well as the progressive disappearance of epidote, titanite and kyanite, may be observed within the second (North Sea) to third km of burial depth (Gulf of Mexico and Bay of Bengal).

Minerofacies 4

moderate-deep burial (*garnet zone*; indicatively Q/QFL% 80 ± 15; tHMC 0.3 ± 0.2, SRD 2.66 ± 0.02, tHM/H% 20 - 40, ZTR 50 ± 20). Orogenic sediments buried at depths between ~ 2 and 4 km are commonly dominated by garnet. In such a depth range, durable minerals including zircon, tourmaline, rutile, and apatite all increase in relative abundance, and may become dominant in anorogenic sediments where garnet is less common. Cr-spinel is concentrated if mafic arc lavas, continental flood basalts, mantle serpentinites, or sandstones derived from such mafic/ultramafic

rocks were present in the source area. Chloritoid or monazite, if originally present, may also relatively increase. Staurolite, instead, is progressively dissolved and finally leached out within the third (North Sea) or fourth km of burial depth (Bay of Bengal). Transparent heavy minerals represent a minority of the heavy fraction.

Minerofacies 5

deep burial (*ZTR zone*; indicatively Q/QFL% 85 ± 10; tHMC 0.2 ± 0.2, SRD 2.65 ± 0.02, tHM/H% ≤ 30, ZTR 60 ± 20). The depleted transparent-heavy-mineral assemblage is dominated by zircon, tourmaline, and rutile. Cr-spinel or monazite may be observed with relative frequency in heavy-mineral mounts if mafic/ultramafic or granitoid rocks (or sandstones derived therefrom) were exposed in source areas, respectively. Garnet is rapidly dissolved and its final disappearance is observed within the fourth (North Sea) or fifth km of burial depth (Gulf of Mexico). Chloritoid shows similar behavior.

Minerofacies 6

very deep burial (*ZTR zone*; indicatively Q/QFL% 90 ± 10; tHMC 0.1 ± 0.1, SRD 2.65 ± 0.01, tHM/H% ≤ 20, ZTR 80 ± 10). The strongly depleted transparent-heavy-mineral assemblage is dominated by zircon, tourmaline, and rutile irrespective of provenance. Tourmaline and apatite may start to decrease. Cr-spinel and monazite may be observed.

Minerofacies 7

extremely deep burial (*ZTR zone*; indicatively Q/QFL% 95 ± 5; tHMC < 0.1, SRD 2.65, tHM/H% ≤ 10, ZTR 90 ± 10). The very strongly depleted transparent-heavy-mineral assemblage is reduced to the most durable species only, including zircon, rutile, tourmaline, but also Cr spinel (presence of mafic/ultramafic rocks in source terranes) or apatite (absence of strong weathering conditions in the drainage basin).

9. Conclusion

Failure to recognize the overwhelming effect of intrastratal dissolution in sediments may lead to wrong provenance and paleogeographic interpretations, as documented emblematically by the long-standing controversies on the birth and evolution of the Nile drainage. Chemically labile clinopyroxene derived from Ethiopian flood basalts dominates transparent-heavy-mineral assemblages in modern Nile sediments but it is rarely found in layers as young as the Pleistocene and virtually lacking in older strata. Since Shukri (1950), its reported absence from sediments buried only a few tens of meters has been widely interpreted as a proof that a long Nile River connected with Ethiopian highlands could not have existed before very recent times. Careful inspection of petrographic and heavy-mineral trends in the offshore Nile Delta succession, however, indicates a progressive exponential loss of unstable minerals with depth, until Oligocene strata consist of pure quartz sand containing a strongly depleted transparent-heavy-mineral suite dominated by durable zircon, tourmaline, rutile, and apatite. The steady decrease in heavy-mineral concentration is accompanied by another simple tell-tale criterion apt to reveal the mark of intrastratal dissolution, i.e., the relative increase in altered and spurious dense grains, which make the bulk of the heavy fraction in Oligo-Miocene sand, sandy silt, and mud samples. Such gradual unidirectional trends are the unique signature of diagenetic dissolution and cannot be interpreted as primarily reflecting provenance. Mineralogical traces of Ethiopian volcanic provenance, however, are not erased completely. Cr-spinel, the only chemically durable component in mafic rocks, is regularly found with increasing relative frequency in strata as old as the lower Oligocene, and the arrival of Oligocene-aged zircons diagnostic of Ethiopian provenance is documented in strata 27.5 Ma old. The Nile Delta succession was thus deposited by a persistent large paleo-river draining Ethiopian highlands since the Oligocene (Fielding et al., 2018).

Under these premises, we interpreted the observed compositional trends as fundamentally controlled by diagenetic dissolution, which may account for up to 95% of the inter-sample

mineralogical variability. Heavy minerals are inferred to represent no more than 20% of the original assemblage in sediments buried less than ~ 1.5 km, no more than 5% in sediments buried between 1.5 and 2.5 km, and no more than 1% for sediments buried more than 4.5 km. Other factors played a subordinate role. Grain-size control, well documented in the modern Delta where it is mainly related to mixing of windblown Saharan quartz with finer-grained fluvial sediments rich in volcanic detritus, is detected also in lower Pleistocene sediments, and with decreasing degree of certainty in Pliocene and even older deposits. The anomalous concentration of denser heavy minerals observed in a few sand samples is ascribed to the selective entrainment of slow-settling grains by contouritic currents. Detailed inferences concerning paleoclimatic changes or paleotectonic events within the paleo-Nile basin, however, cannot be drawn with any certainty based on mineralogical modes so deeply affected by diagenetic bias.

The reported evidence in favor of dominant diagenetic control is consistent with what observed in Cenozoic stratigraphic sections deposited in diverse geodynamic settings worldwide, and allows us to interpret the superposed petrofacies and minerofacies identified in the offshore Nile Delta succession as diagenetic suites, fundamentally controlled by the different chemical stability of detrital minerals.

Acknowledgments

Samples from the Cenozoic Nile Delta succession were kindly provided by BP Egypt as part of NERC-BP CASE PhD Studentship NE/I018433/1 to Fielding. Pre-Aswan-High-Dam Nile samples were retrieved from the Geological Museum of the Fouad I University at Cairo thanks to Ahmed El Kammar and Ibtsam Arafa. Modern Nile and Nile Delta samples were collected with the precious assistance in the field by Lilly Bau, Cecilia Leo, and Ada Ali Abdel Megid. We heartily thank Marta Padoan and Giovanni Vezzoli (University of Milano-Bicocca) for fundamental help in heavy-mineral and petrographic analyses, and Peter Butterworth (BP),

Benjamin Kneller (University of Aberdeen), and Ian Millar (British Geological Survey) for precious advice. Reviewers Kitty Milliken, #2, and Luiz Fernando De Ros plus Editor Andrew Miall generously provided very helpful constructive criticism.

References

Abdelkareem, M., Ghoneim, E., El-Baz, F., Askalany, M., 2012. New insight on paleoriver development in the Nile basin of the eastern Sahara. Journal of African Earth Sciences, 62, 35-40.

Adamson, D., Williams, F., 1980. Structural geology, tectonics and the control of drainage in the Nile basin. In: M.A.J. Williams, H. Faure (Eds.), The Sahara and the Nile, Rotterdam, Balkema, Rotterdam, pp. 225-252.

Adamson, D., McEvedy, R., Williams, M.A.J., 1993. Tectonic inheritance in the Nile basin and adjacent areas. Israel Journal of Earth Sciences 41, 75-85.

Ager, D.,V., 1981. The nature of the stratigraphical record. Halsted Press, New York, 122 p.

Ando, S., Garzanti, E., 2014. Raman spectroscopy in heavy-mineral studies. Geological Society of London Special Publication 386, 395-412.

Andò, S., Garzanti, E., Padoan, M., Limonta, M., 2012. Corrosion of heavy minerals during weathering and diagenesis: a catalogue for optical analysis. Sedimentary Geology, 280, 165-178.

Bartolini, C., Malesani, P.G., Manetti, P., Wezel, F.C., 1975. Sedimentology and petrology of Quaternary sediments from the Hellenic Trench, Mediterranean Ridge and the Nile Cone from D.S.D.P., Leg 13, cores. Sedimentology 22, 205-236.

Bateman, R.M., Catt, J.A., 2007. Provenance and palaeoenvironmental interpretation of superficial deposits, with particular reference to post-depositional modification of heavy mineral assemblages. In: Mange, M.A., Wright, D.T. (Eds), Heavy Minerals in Use. Elsevier, Amsterdam, Developments in Sedimentology, 58, 151-188.

Berry, L., Whiteman, A.J., 1968. The Nile in the Sudan. The Geographical Journal, 134, 1-33.

Blatt, H., Sutherland, B., 1969. Intrastratal solution and non-opaque heavy minerals in mudrocks. Journal of Sedimentary Petrology, 39, 591-600.

Bornhauser, M., 1940. Heavy mineral associations in quaternary and late tertiary sediments of the Gulf Coast of Louisiana and Texas. Journal of Sedimentary Petrology, 10, 125-135.

Bowman, T.S. 1931. Report on boring for oil in Egypt. Section III: Eastern Desert and adjoining islands. Egypt, Mines and Quarries Department.

Box, M.R., Krom, M.D, Cliff, R.A., Bar-Matthews, M., Almogi-Labin, A., Ayalon, A., Paterne, M., 2011. Response of the Nile and its catchment to millennial-scale climatic change since the LGM from Sr isotopes and major elements of East Mediterranean sediments. Quaternary Science Reviews, 30, 431-442

Bramlette, M.N., 1941. The stability of minerals in sandstone. Journal of Sedimentary Petrology, 11, 32-36.

Burke, K., Wells, G.L., 1989. Trans-African drainage system of the Sahara: was it the Nile? Geology, 17, 743-747.

Butzer, K.W., Hansen, C.L., 1968. Desert and River in Nubia: geomorphology and prehistoric environments at the Aswan Reservoir. University of Wisconsin Press, Madison, Wisconsin, 562 pp.

Cawood, P.A., 1983. Modal composition and detrital clinopyroxene geochemistry of lithic sandstones from the New England Fold Belt (east Australia): A Paleozoic forearc terrane. Geological Society of America Bulletin, 94, 1199-1214.

Chumakov, I.S., 1968. Pliocene ingression in the Nile Valley according to new data. In: Butzer, K.W., Hansen, C.L. (Eds.), Desert and River in Nubia, Geomorphology and Prehistoric Environments at the Aswan Reservoir, The University of Wisconsin Press, Madison, pp. 521-522.

Cibin, U., Cavazza, W., Fontana, D., Milliken, K.L., McBride, E.F., 1993. Comparison of composition and texture of calcite-cemented concretions and host sandstones, Northern Apennines, Italy. Journal of Sedimentary Research, 63, 945-954.

Cogen, W.M., 1940. Heavy-mineral zones of Louisiana and Texas Gulf coast sediments. American Association of Petroleum Geologists Bulletin 24, 2069-2101.

Comas-Cufí, M., Thió-Henestrosa, F.S., CoDaPack 2.0: a stand-alone, multi-platform compositional software.

Cox, K.G., 1989. The role of mantle plumes in the development of continental drainage patterns. Nature, 342, 873-877.

Craig, J., Grigo, D., Rebora, A., Serafini, G., Tebaldi, E. 2011. From Neoproterozoic to early Cenozoic: exploring the potential of older and deeper hydrocarbon plays across North Africa and the Middle East. In: Vining, B.A., Pickering, S.C. (Eds.), Petroleum Geology, from Mature Basins to New Frontiers - Proceedings of the 7th Petroleum Geology Conference, Geological Society London, pp. 673-705.

Dickinson, W.R., Rich, E.I., 1972. Petrologic intervals and petrofacies in the Great Valley sequence, Sacramento Valley, California. Geological Society of America Bulletin, 83, 3007-3024.

Dolson, J. C., Boucher, P.J., Siok, J., Heppard, P.D., 2005. Key challenges to realizing full potential in an emerging giant gas province: Nile Delta/Mediterranean offshore, deep water, Egypt. In: Doré,

A.G., Vining, B.A. (Eds), Petroleum Geology: North-West Europe and Global Perspectives - Proceedings of the 6th Petroleum Geology Conference, Geological Society London, pp. 607-624.

Dolson, J.C., El Barkooky, A., Wehr, F., Gingerich, D., Procharza, N., Shann, M. 2002. The Eocene and Oligocene palaeo-geography of Whale Valley and the Fayoum basins, implications for hydrocarbon exploration in the Nile Delta and eco-tourism in the Greater Fayoum basin. In: Cairo 2002. American Association of Petroleum Geologists/EPEX/SEG/EGS/EAGE Field Trip Notes No.7.

El Sisi, Z.A., Sharaf, L.N., Dawood, Y.H., Hassouba, A.B. 1997. Source of clastic supply to the Sidi Salem and Abu Madi reservoirs of the Nile Delta, a Provenance Study. In: 13th Egyptian General Petroleum Congress, 291-295.

Evans, T.R., Coleman, N.C., 1974. North Sea geothermal gradients. Nature, 247, 28-30.

Fielding, L., Najman, Y., Millar, I., Butterworth, P., Andò, S., Padoan, M., Barfod, D., Kneller, B., 2017. A detrital record of the Nile River and its catchment. Journal of the Geological Society London, 174, 301-317.

Fielding, L., Najman, Y., Millar, I., Butterworth, P., Garzanti, E., Vezzoli, G., Barfod, D., Kneller, B., 2018. The initiation and evolution of the river Nile. Earth and Planetary Science Letters, 489, 166-178.

France-Lanord, C., Derry, L., Michard, A., 1993. Evolution of the Himalaya since Miocene time: isotopic and sedimentological evidence from the Bengal Fan. Geological Society London, Special Publications, 74, 603-621.

Gabriel, K.R., 1971. The biplot graphic display of matrices with application to principal component analysis. Biometrika, 58, 453-467.

Galehouse, J.S., 1971. Point counting. In: Carver, R.E. (Ed.), Procedures in sedimentary petrology. Wiley, New York, pp. 385-407

Gani, N.D.S., Gandi, M.R., Abdelsalam, M.G.., 2007. Blue Nile incision on the Ethiopian Plateau: pulsed plateau growth, Pliocene uplift, and hominin evolution. GSA Today, 17(9), 4-11.

Garzanti, E., 2016, From static to dynamic provenance analysis - Sedimentary petrology upgraded: Sedimentary Geology, 336, 3-13.

Garzanti, E., 2017. The maturity myth in sedimentology and provenance analysis. Journal of Sedimentary Research, 87, 353-365.

Garzanti, E., Andò, S., 2007a. Heavy-mineral concentration in modern sands: implications for provenance interpretation. In: Mange, M.A., Wright, D.T. (Eds.), Heavy Minerals in Use. Elsevier, Amsterdam, Developments in Sedimentology, Series 58, 517-545.

Garzanti, E., Andò, S., 2007b. Plate tectonics and heavy-mineral suites of modern sands. In: Mange, M.A., Wright, D.T. (Eds.), Heavy Minerals in Use, Developments in Sedimentology Series, 58. Elsevier, Amsterdam, pp. 741-763.

Garzanti, E., Malusà, M.G., 2008. The Oligocene Alps: Domal unroofing and drainage development during early orogenic growth. Earth and Planetary Science Letters, 268, 487-500.

Garzanti E., Ando' S., Vezzoli G., Ali Abdel Megid A., El Kammar A., 2006. Petrology of Nile River sands (Ethiopia and Sudan): sediment budgets and erosion patterns. Earth and Planetary Science Letters, 252, 327-341.

Garzanti E., Andò, S., Vezzoli G., 2009, Grain-size dependence of sediment composition and environmental bias in provenance studies, Earth and Planetary Science Letters, 277, 422-432.

Garzanti, E., Andò, S., France-Lanord, C., Vezzoli, G., Galy, V., Najman, Y., 2010. Mineralogical and chemical variability of fluvial sediments. 1. Bedload sand (Ganga-Brahmaputra, Bangladesh). Earth and Planetary Science Letters 299, 368-381.

Garzanti, E., Andò, S., France-Lanord, C., Galy, V., Censi, P., Vignola, P., 2011. Mineralogical and chemical variability of fluvial sediments. 2. Suspended-load silt (Ganga-Brahmaputra, Bangladesh). Earth and Planetary Science Letters, 302, 107-120.

Garzanti, E., Padoan, M., Andò, S., Resentini, A., Vezzoli, G., Lustrino, M., 2013a. Weathering and relative durability of detrital minerals in equatorial climate: sand petrology and geochemistry in the East African Rift. The Journal of Geology 121, 547-580.

Garzanti, E., Padoan, M., Setti, M., Peruta, L., Najman, Y., Villa, I.M., 2013b. Weathering geochemistry and Sr-Nd fingerprints of equatorial upper Nile and Congo muds. Geochemistry, Geophysics, Geosystems, 14, 292-316

Garzanti, E., Andò, S., Padoan, M., Vezzoli, G., El Kammar, A., 2015. The modern Nile sediment system: processes and products. Quaternary Science Reviews, 130, 9-56

Garzanti, E., Vermeesh, P., Rittner, M., Simmons, M., 2018a. The zircon story of the Nile: time-structure maps of source rocks and discontinuous propagation of detrital signals. Basin Research, in press.

Garzanti E., Dinis, P., Vermeesch, P., Andò, S., Hahn, A., Huvi, J., Limonta, M., Padoan, M., Resentini, A., Rittner, M., Vezzoli, G., 2018b. Dynamic uplift, recycling, and climate control on the petrology of passive-margin sand (Angola). Sedimentary Geology, https://doi.org/10.1016/j.sedgeo.2017.12.009.

Gazzi, P., 1965. On the heavy mineral zones in the geosyncline series, recent studies in the Northern Apennines, Italy. Journal of Sedimentary Petrology, 35, 109-115.

Goudie, A.S., 2005. The drainage of Africa since the Cretaceous. Geomorphology 67, 437-456.

Gould, S.J., 1987. Time's arrow, time's cycle: Myth and metaphor in the discovery of geological time. Harvard University Press, Cambridge, 222 p.

Griffin, D.L. 2002. Aridity and humidity, two aspects of the Late Miocene climate of North Africa and the Mediterranean. Palaeogeography, Palaeoclimatology, Palaeoecology, 182, 65-91.

Hassan, F.A., 1976. Heavy minerals and the evolution of the modern Nile. Quaternary Research, 6, 425-444.

Hereher, M.E., 2010. Sand movement patterns in the Western Desert of Egypt: an environmental concern. Environmental Earth Sciences 59, 1119-1127.

Hereher, M.E., 2014. Assessment of sand drift potential along the Nile Valley and Delta using climatic and satellite data. Applied Geography 55, 39-47.

Hubert, J.F., 1962. A zircon-tourmaline-rutile maturity index and the interdependence of the composition of heavy minerals assemblages with the gross composition and texture of sandstones. Journal of Sedimentary Petrology, 32, 440-450.

Ingersoll, R.V., Bullard, T.F., Ford, R.L., Grimm, J.P., Pickle, J.D., Sares, S.W., 1984. The effect of grain size on detrital modes: a test of the Gazzi–Dickinson point-counting method. Journal of Sedimentary Petrology, 54, 103-116.

Issawi, B., McCauley, J.F., 1992. The Cenozoic rivers of Egypt: the Nile problem. In: Friedman, R. F., Adams, B. (eds.), The Followers of Horus, studies dedicated to Michael Allen Hoffman1944-1990, Oxbow Monograph, 20, 121-138.

Issawi, B., Osman, R., 2008. Egypt during the Cenozoic: geological history of the Nile River. Bulletin of the Tethys geological society, 3, 43-62.

Johnsson, M., 1993. The system controlling the composition of clastic sediments. In Johnsson, M. J., Basu, A. (Eds.), Processes controlling the composition of clastic sediments. Geological Society of America, Special Paper 284, pp. 1-19.

Kahneman, D., 2011. Thinking, fast and slow. Penguin, London, 499 p.

Komar, P.D., 2007. The entrainment, transport and sorting of heavy minerals by waves and currents In: Mange, M.A., Wright, D.T. (Eds.), Heavy minerals in use. Elsevier, Amsterdam, Developments in Sedimentology Series, 58, pp. 3-48.

Leila, M., Moscariello, A., Šegvić, B., 2018. Geochemical constraints on the provenance and depositional environment of the Messinian sediments, onshore Nile Delta, Egypt: Implications for the late Miocene paleogeography of the Mediterranean. Journal of African Earth Sciences, 143, 215-241.

Limonta, M., Garzanti, E., Resentini, A., Andò, S., Boni, M., Bechstädt, T., 2015. Multicyclic sediment transfer along and across convergent plate boundaries (Barbados, Lesser Antilles). Basin Research, 1-18, DOI: 10.1111/bre.12095.

Limonta, M., Resentini, A., Carter, A., Bandopadhyay, P.C., Garzanti, E., 2017. Provenance of Oligocene Andaman sandstones (Andaman–Nicobar Islands): Ganga–Brahmaputra or Irrawaddy derived?. Geological Society London, Memoirs, 47, 141-152.

Limonta, M., Garzanti, E., Andò, S., Carter, A., Milliken, K.L., Pickering, K.T., 2018. Mineralogy of Nicobar Fan turbidites (IODP Leg 362): Himalayan provenance and diagenetic control. EGU General Assembly Conference Abstracts, v. 20, EGU2018-7117.

Macgregor, D.S., 2012. The development of the Nile drainage system: integration of onshore and offshore evidence. Petroleum Geoscience, 18, 417-431.

Mange, A., Maurer, H.F.W. 1992. Heavy minerals in colour. London, Chapman and Hall, 147 p.

McBride, E.F. 1985. Diagenetic processes that affect provenance determinations in sandstones. In: Zuffa, G. G. (Ed.), Provenance of arenites. Dordrecht, Reidel Publ., NATO ASI Series, 148, 95-113.

McCauley, J.F., Breed, C.S., Schaber, G.G., McHugh, W.P., Issawi, B., Haynes, C.V., Grolier, M.J., El Kilani, A., 1986. Paleodrainages of the eastern Sahara - The radar rivers revisited (SIR-A/B implications for a mid-Tertiary trans-African drainage system). Institute of Electrical and Electronics Engineers Transactions on Geoscience and Remote Sensing, GE-24, 624-648.

McDougall, I., Morton, W.H., Williams, M.A.J., 1975. Age and rates of denudation of Trap Series basalts at Blue Nile Gorge, Ethiopia. Nature, 254, 207-209.

Milliken, K.L., 1988. Loss of provenance information through subsurface diagenesis in Plio-Pleistocene sandstones, Gulf of Mexico. Journal of Sedimentary Petrology, 58, 992-1002.

Milliken, K.L., 1992. Chemical behavior of detrital feldspars in mudrocks versus sandstones, Frio Formation (Oligocene), South Texas. Journal of Sedimentary Petrology, 62, 790-801.

Milliken, K.L., 2003. Late diagenesis and mass transfer in sandstone shale sequences. In: Mackenzie, F.T. (Ed.), Treatise on Geochemistry. Elsevier Pergamon, Oxford UK, pp. 159-190 pp.

Milliken, K.L., 2007. Provenance and diagenesis of heavy minerals, Cenozoic units of the northwestern Gulf of Mexico sedimentary basin In: Mange, M.A. and Wright, D.T. (Eds.), Heavy Minerals in Use. Elsevier, Amsterdam, Developments in Sedimentology Series 58, pp. 247-261.

Milliken, K.L., McBride, E.F., Land, L.S., 1989. Numerical assessment of dissolution versus replacement in the subsurface destruction of detrital feldspars, Oligocene Frio Formation, South Texas. Journal of Sedimentary Petrology, 59, 740-757.

Morton, A., Mundy, D., Bingham, G., 2012. High-frequency fluctuations in heavy mineral assemblages from Upper Jurassic sandstones of the Piper Formation, UK North Sea: relationships with sea-level change and floodplain residence. Geological Society of America Special Papers, 487, 163-176.

Morton, A.C., Hallsworth, C.R., 1999. Processes controlling the composition of heavy mineral assemblages in sandstones. Sedimentary Geology, 124, 3-29.

Morton, A.C., Hallsworth, C., 2007. Stability of detrital heavy minerals during burial diagenesis. In: Mange, M.A. and Wright, D.T. (Eds.), Heavy Minerals in Use. Elsevier, Amsterdam, Developments in Sedimentology Series 58, pp. 215-245.

Morton, A.C., Meinhold, G., Howard, J.P., Phillips, R.J., Strogen, D., Abutarruma, Y., Elgadry, M., Thusu, B., Whitham, A.G., 2011. A heavy mineral study of sandstones from the eastern Murzuq Basin, Libya: Constraints on provenance and stratigraphic correlation. Journal of African Earth Sciences, 61, 308-330.

Moucha, R., Forte, A.M., 2011. Changes in African topography driven by mantle convection. Nature Geosciences 4, 707-712.

Nachmias, J., 1969. Source rocks of Saqiye Group sediments in coastal plain of Israel - a heavy mineral study. Israel Journal of Earth Sciences, 18, XXX.

Najman, Y., Bickle, M., BouDagher-Fadel, M., Carter, A., Garzanti, E., Paul, M., Wijbrans, J., Willett, E., Oliver, G., Parrish, R., Akhter, S.H., Allen, R., Andò, S., Chisty, E., Reisberg, L., Vezzoli, G., 2008. The Paleogene record of Himalayan erosion: Bengal Basin, Bangladesh. Earth and Planetary Science Letters, 273, 1-14.

Najman, Y., Allen, R., Willett, E.A.F., Carter, A., Barfod, D., Garzanti, E., Wijbrans, J., Bickle, M., Vezzoli, G., Andò, S., Oliver, G., Uddin, M.J., 2012. The record of Himalayan erosion preserved in the sedimentary rocks of the Hatia Trough of the Bengal Basin and the Chittagong Hill Tracts, Bangladesh. Basin Research, 24, 499-519.

Nechaev, V.P., Isphording, W.C., 1993. Heavy mineral assemblages of continental margins as indicators of plate-tectonic environments. Journal of Sedimentary Petrology 63, 1110-1117.

Nie J., Peng W., Pfaff K., Möller A., Garzanti E., Andò S., Stevens T., Bird A., Chang H., Song Y., Liu S., Ji S. 2013. Controlling factors on heavy mineral assemblages in Chinese loess and Red Clay. Palaeogeography, Palaeoclimatology, Palaeoecology, 381-382, 110-118.

Nyssen, J., Poesen, J., Moeyersons, J., Deckers, J., Haile, M., Lang, A., 2004. Human impact on the environment in the Ethiopian and Eritrean highlands—a state of the art. Earth-science reviews, 64, 273-320.

Nyssen, J., Poesen, J., Moeyersons, J., Haile, M., Deckers, J., 2008. Dynamics of soil erosion rates and controlling factors in the Northern Ethiopian Highlands – towards a sediment budget. Earth Surface Processes and Landforms 33, 695-711.

Pettijohn, F.J., 1941. Persistence of heavy minerals and geologic age. The Journal of Geology, 1941, 49, 610-625.

Pickford, M., Wanas, H., Soliman, H. 2006. Indications for a humid climate in the Western Desert of Egypt 11–10 Myr ago, evidence from Galagidae (Primates, Mammalia). Comptes Rendus Palevol, 5, 935-943.

Pik, R., Marty, B., Carignan, J., Lavé, J., 2003. Stability of the Upper Nile drainage network (Ethiopia) deduced from (U–Th)/He thermochronometry: implications for uplift and erosion of the Afar plume dome. Earth and Planetary Science Letters, 215, 73-88.

Popper, K., 1959, The logic of scientific discovery. Hutchinson & Co, London, 480 p.

Riad, S., Abdelrahman, E.M., Refai, E., El-Ghalban, H.M., 1989. Geothermal studies in the Nile Delta, Egypt. Journal of African Earth Sciences, 9, 637-649.

Roskin, J., Katra, I., Blumberg, D.G., 2014. Particle-size fractionation of eolian sand along the Sinai-Negev erg of Egypt and Israel. Geological Society of America Bulletin 126, 47-65.

Said, R., 1993. The River Nile: geology, hydrology and utilization. Pergamon, Oxford, 320 p.

Salama, R.B., 1987. The evolution of the River Nile. The buried saline rift lakes in Sudan – I. Bahr El Arab Rift, the Sudd buried saline lake. Journal of African Earth Sciences, 6, 899-913.

Salama, R.B., 1997. Rift basins of the Sudan. Sedimentary Basins of the World 3, 105-149.

Salem, A.M., Ketzer, J.M., Morad, S., Rizk, R.R., Al-Aasm, I.S., 2005. Diagenesis and reservoir-quality evolution of incised-valley sandstones: evidence from the Abu Madi gas reservoirs (Upper Miocene), The Nile Delta Basin, Egypt. Journal of Sedimentary Research, 75, 572-584.

Samuel, A., Kneller, B., Raslan, S., Sharp, A., Parsons, C., 2003. Prolific deep-marine slope channels of the Nile Delta, Egypt. American Association of Geologists Bulletin, 87, 541-560.

Sandford, K.S., Arkell, W.J., 1939. Paleolithic man and the Nile Valley in Lower Egypt. Pre-historic Survey of Egypt and Western Asia, vol. IV., University of Chicago Oriental Institute, Publication XLVI.

Schull, T.J., 1988. Rift basins of interior Sudan: petroleum exploration and discovery. American Association of Petroleum Geologists Bulletin 72, 1128-1142.

Sharp, J.M., Galloway, W.E., Land, L.S., McBride, E.F., Blanchard, P.E., Bodner, D.P., Dutton, S.P., Farr, M.R., Gold, P.B., Jackson, T.J., Lundegard, P.D., Macpherson, G.L., Milliken, K.L., 1988. Diagenetic processes in Northwest Gulf of Mexico sediments. In: Chilingarian, G.V. and Wolf, K.H. (Eds.), Diagenesis II. Elsevier, Amsterdam, Developments in Sedimentology Series 43, pp. 43-133.

Shukri, N.M., 1950. The mineralogy of some Nile sediments. Quart. J. Geol. Soc. London, 105, 511-534.

Slingerland, R., 1984. Role of hydraulic sorting in the origin of fluvial placers. J. Sedim. Petrol. 54, 137-150.

Stow, D.A.V., Lovell, J.P.B., 1979. Contourites: their recognition in modern and ancient sediments. Earth-Science Reviews, 14, 251-291.

Sutcliffe, J.V., Parks, Y.P., 1999. The Hydrology of the Nile. International Association of Hydrological Sciences, Special Publication 5, 179 p.

Szulc, A.G., Najman, Y., Sinclair, H. D., Pringle, M., Bickle, M., Chapman, H., Garzanti, E., Andò, S., Huyghe, P., Mugnier, J.L., Ojha, T., DeCelles, P., 2006. Tectonic evolution of the Himalaya constrained by detrital ^{40}Ar–^{39}Ar, Sm–Nd and petrographic data from the Siwalik foreland basin succession, SW Nepal. Basin Research, 18, 375-391.

Talbot, M.R., Williams, M.A.J., 2009. Cenozoic evolution of the Nile Basin. In: Dumont, H.J. (ed.), The Nile – Origin, environments, limnology and human use. Springer, The Netherlands, pp. 37-60.

Underwood, C.J., King, C., Steurbaut, E., 2013. Eocene initiation of Nile drainage due to East African uplift. Palaeogeography, Palaeoclimatology, Palaeoecology, 392, 138-145.

Van Loon, A.J., Mange, M.A., 2007. 'In situ' dissolution of heavy minerals through extreme weathering, and the application of the surviving assemblages and their dissolution characteristics to correlation of Dutch and German silver sands. In: Mange, M.A., Wright, D.T. (Eds), Heavy Minerals in Use. Elsevier, Amsterdam, Developments in Sedimentology, 58, 189-213.

Velbel, M.A., 1993. Formation of protective surface layers during silicate-mineral weathering under well-leached, oxidizing conditions. American Mineralogist, 78, 405-405.

Vermeersch, P. M., Van Neer, W., 2015. Nile behaviour and Late Palaeolithic humans in upper Egypt during the Late Pleistocene. Quaternary Science Reviews, 130, 155-167.

Vögeli, N., Huyghe, P., van der Beek, P., Najman, Y., Garzanti, E., Chauvel, C., 2018. Weathering regime in the Eastern Himalaya since the mid-Miocene: indications from detrital geochemistry and clay mineralogy of the Kameng River Section, Arunachal Pradesh, India. Basin Research, 30, 59-74.

von Eynatten, H., Dunkl, I., 2012. Assessing the sediment factory: the role of single grain analysis. Earth-Science Reviews 115, 97-120.

von Eynatten, H., Pawlowsky-Glahn, V., Egozcue, J.J., 2002. Understanding perturbation on the simplex: a simple method to better visualise and interpret compositional data in ternary diagrams. Mathematical Geology, 34, 249-257.

Wang, J.G., Wu, F.Y., Garzanti, E., Hu, X., Ji, W.Q., Liu, Z.C., Liu, X.C., 2016. Upper Triassic turbidites of the northern Tethyan Himalaya (Langjiexue Group): the terminal of a sediment-routing system sourced in the Gondwanide Orogen. Gondwana Research, 34, 84-98.

Williams, M.A.J., Talbot, M.R., 2009. Late Quaternary environments in the Nile basin. In: Dumont, H.J. (ed.), The Nile – Origin, environments, limnology and human use. Springer, The Netherlands, pp. 61-72.

Williams, M.A.J., Adamson, D., Prescott, J.R., Williams, F.M., 2003. New light on the age of the White Nile. Geology 31, 1001-1004.

Williams, M.A.J., Williams, F.M., Duller, G.A.T., Munro, R.N., El Tom, O.A.M., Barrows, T.T., Macklin, M., Woodward, J., Talbot, M.R., Haberlah, D, Fluin, J., 2010. Late Quaternary floods and droughts in the Nile valley, Sudan: new evidence from optically stimulated luminescence and AMS radiocarbon dating. Quaternary Science Reviews, 29, 1116-1137.

Williams, M.A.J., Duller, G.A.T., Williams, F.M., Woodward, J.C., Macklin, M.G., El Tom, O.A.M., Munro, R.N., El Hajaz, Y., Barrows, T. T., 2015. Causal links between Nile floods and eastern Mediterranean sapropel formation during the past 125 kyr confirmed by OSL and radiocarbon dating of Blue and White Nile sediments. Quaternary Science Reviews, 130, 89-108.

Woodward, J.C., Williams, M.A.J., Garzanti, E., Macklin, M.G., Marriner, N., 2015. From source to sink: exploring the Quaternary history of the Nile. Quaternary Science Reviews, 130, 3-8.

Zaghloul, Z.M., El-Shahat, A., Hegab, O., Kora, M.A.M., 1980. Mineralogy of the Tertiary-Quaternary subsurface sediments, west Nile Delta area. Egyptian Journal of Geology, 24, 177-188.

Table 1. Main parameters defining the petrographic composition of Oligocene to modern Nile Delta and Nile River sand (mean values in **bold**, standard deviations in *italics*). N° = number of samples; Q = quartz; KF = K-feldspars; P = plagioclase; L = lithic grains (Lvm = volcanic and metavolcanic; Lc = carbonate; Lsm = sedimentary and metasedimentary); HM = heavy minerals.

	N°	Q	KF	P	Lvm	Lc	Lsm	mica	HM	total
Pre-AHD Nile										
Very fine sand	3	**43**	**6**	**11**	**22**	**1.2**	**4**	**1.3**	**12**	100.0
		5	*2*	*1*	*5*	*0.5*	*4*	*0.9*	*3*	
Fine sand	2	**68**	**5**	**9**	**10**	**0**	**2**	**0.1**	**5**	100.0
		6	*3*	*3*	*0*	*0*	*0*	*0.2*	*0*	
Modern Nile										
Silty levees	8	**30**	**3**	**18**	**31**	**1**	**3**	**1.1**	**12**	100.0
		8	*1*	*5*	*12*	*1*	*3*	*0.8*	*9*	
Sand bars	11	**66**	**5**	**10**	**10**	**1**	**3**	**0.3**	**5**	100.0
		9	*2*	*3*	*4*	*1*	*2*	*0.3*	*3*	
Delta beaches	9	**65**	**7**	**7**	**7**	**0.6**	**4**	**0.6**	**9**	100.0
		10	*3*	*3*	*4*	*0.6*	*4*	*0.4*	*5*	
Delta dunes	2	**78**	**5**	**7**	**5**	**0.2**	**0.5**	**0.2**	**4**	100.0
		15	*2*	*3*	*6*	*0.2*	*0.4*	*0.3*	*3*	
Cenozoic succession										
Lower Pleistocene	2	**76**	**5**	**9**	**3**	**0**	**1**	**0.4**	**6**	100.0
		14	*0*	*4*	*4*	*0*	*1*	*0.6*	*4*	
Pliocene	5	**83**	**5**	**7**	**3**	**0.1**	**0.3**	**0.6**	**2**	100.0
		6	*1*	*3*	*2*	*0.1*	*0.4*	*0.5*	*1*	
Miocene	5	**89**	**2**	**7**	**2**	**0**	**0.3**	**0.2**	**0.3**	100.0
		3	*1*	*2*	*1*	*0*	*0.4*	*0.2*	*0.5*	
Aquitanian	2	**88**	**2**	**8**	**2**	**0.1**	**1**	**0**	**0.3**	100.0
		2	*1*	*2*	*1*	*0.2*	*0*	*0*	*0.0*	
Oligocene	2	**96**	**0.4**	**2**	**2**	**0.1**	**0.1**	**0**	**0.3**	100.0
		1	*0.2*	*0*	*1*	*0.1*	*0.1*	*0*	*0.4*	

Table 2. Heavy-mineral assemblages in Oligocene to modern Nile Delta and Nile River sand and mud (mean values in **bold**, standard deviations in *italics*). N° = number of samples; ZTR = zircon + tourmaline + rutile; &tHM = other transparent heavy minerals, including pumpellyite, chloritoid, andalusite, and sillimanite); tHMCw% = transparent-heavy-mineral concentration in weight; tHM/Hw% = ratio between the amount of transparent heavy minerals and the total weight of the heavy fraction.

	N°	zircon	tourmaline	rutile	titanite	apatite	monazite	epidote	garnet	staurolite	kyanite	amphiboles	pyroxene	Cr-spinel	olivine	&tHM	Total	ZTR	tHMC w%	tHM / Hw%
Pre-AHD Nile	10	**0.4**	**0.1**	**0.1**	**1**	**1**	**---**	**15**	**1**	**0.2**	**---**	**22**	**59**	**---**	**1**	**0.1**	100.0	**1**	**6**	**75%**
					1	*1*		*8*	*1*			*9*	*15*		*1*			*1*	*7*	*15%*
Modern Nile																				
Silty levee sand	8	**0.3**	**0.2**	**0.2**	**0.2**	**0.2**	**---**	**17**	**0.4**	**0.1**	**0.1**	**18**	**62**	**0.1**	**1**	**---**	100.0	**1**	**11**	**68%**
								4				*5*	*8*		*1*			*1*	*4*	*7%*
Sand bars	8	**1**	**0.1**	**0.4**	**1**	**---**	**0.1**	**20**	**1**	**---**	**0.1**	**22**	**54**	**---**	**0.2**	**0.1**	100.0	**1**	**8**	**75%**
		1			*1*			*6*	*1*			*6*	*5*					*1*	*3*	*6%*
Delta beaches	9	**1**	**0.3**	**0.2**	**0.4**	**0.1**	**0.1**	**21**	**1**	**0.3**	**0.1**	**30**	**46**	**---**	**---**	**0.1**	100.0	**1**	**6**	**79%**
		1						*7*	*2*			*8*	*7*					*2*	*3*	*15%*
Delta dunes	2	**0.1**	**1**	**---**	**1**	**1**	**---**	**22**	**2**	**1**	**0.2**	**42**	**29**	**---**	**---**	**0.2**	100.0	**2**	**5**	**81%**
			2		*0*	*0*		*9*	*1*	*2*		*6*	*9*					*2*	*3*	*5%*
Lower Pleistocene																				
Mud	2	**1**	**0.2**	**1**	**1**	**3**	**---**	**46**	**2**	**0.2**	**---**	**46**	**0.2**	**---**	**---**	**---**	100.0	**2**	**5**	**51%**
		0		*0*	*0*	*0*		*2*	*0*			*1*						*1*	*6*	*11%*
Silty sand	2	**1**	**0.5**	**1**	**0.5**	**2**	**---**	**46**	**1**	**0.6**	**0.7**	**47**	**---**	**---**	**---**	**---**	100.0	**2**	**2**	**52%**
		1		*1*		*4*		*4*	*1*	*0.8*	*0.6*	*6*						*1*	*1*	*12%*
Sand	2	**5**	**1**	**1**	**1**	**2**	**---**	**41**	**2**	**0.7**	**---**	**45**	**1**	**---**	**---**	**---**	100.0	**7**	**3**	**57%**
		2	*0*	*0*	*0*	*0*		*2*	*1*	*0.3*		*1*	*1*					*1*	*3*	*18%*
Pliocene																				
Mud	5	**2**	**3**	**2**	**5**	**8**	**---**	**69**	**1**	**0.3**	**---**	**10**	**---**	**0.2**	**---**	**---**	100.0	**7**	**1.7**	**20%**
		3	*3*	*2*	*7*	*5*		*13*	*1*			*9*						*7*	*1.1*	*15%*
Sandy silt	2	**11**	**6**	**15**	**---**	**9**	**---**	**48**	**5**	**0.2**	**0.2**	**5**	**---**	**0.5**	**---**	**---**	100.0	**32**	**0.7**	**25%**

		14	*8*	*18*		*1*		*43*	*7*			*7*						*40*	*0.6*	*12%*
Sand	5	**13**	**3**	**5**	**4**	**4**	**0.4**	**44**	**7**	**3**	**1**	**15**	**---**	**---**	**---**	**---**	100.0	**21**	**0.7**	**46%**
		10	*3*	*5*	*2*	*1*		*9*	*3*	*2*	*1*	*18*						*17*	*0.5*	*16%*
Langhian-Burdigalian																				
Mud	1	42	13	15	0.4	16	---	4	8	---	---	---	---	2	---	---	100.0	69	0.2	3%
Sandy silt	2	**31**	**22**	**25**	**---**	**10**	**---**	**7**	**5**	**---**	**---**	**---**	**---**	**---**	**---**	**---**	100.0	**78**	**0.1**	**5%**
		8	*9*	*6*		*8*		*12*	*4*									*7*	*0.1*	*5%*
Sand	5	**44**	**11**	**17**	**2**	**11**	**1**	**1**	**12**	**0.2**	**---**	**---**	**0.1**	**1**	**---**	**---**	100.0	**72**	**0.1**	**22%**
		4	*4*	*2*	*1*	*5*	*2*	*1*	*5*					*1*				*5*	*0.1*	*5%*
Aquitanian																				
Mud	2	**32**	**20**	**12**	**---**	**30**	**1**	**1**	**5**	**---**	**---**	**---**	**---**	**0.3**	**---**	**---**	100.0	**63**	**0.1**	**6%**
		5	*1*	*9*		*1*	*1*	*0*	*5*									*5*	*0.0*	*0%*
Sand	2	**44**	**17**	**18**	**1**	**9**	**---**	**1**	**9**	**---**	**---**	**1**	**---**	**0.3**	**---**	**---**	100.0	**79**	**0.1**	**19%**
		14	*4*	*1*	*2*	*3*		*1*	*3*			*1*						*9*	*0.0*	*4%*
Oligocene																				
Mud	2	**46**	**23**	**15**	**---**	**9**	**0.4**	**4**	**2**	**---**	**---**	**---**	**---**	**---**	**---**	**0.4**	100.0	**84**	**0.1**	**5%**
		6	*6*	*11*		*4*		*5*	*2*									*10*	*0.1*	*1%*
Sandy silt	1	68	15	14	---	3	---	---	---	---	---	---	---	---	---	---	100.0	97	0.0	3%
Sand	2	**56**	**10**	**24**	**1**	**6**	**0.5**	**---**	**1**	**---**	**---**	**---**	**---**	**1**	**---**	**---**	100.0	**91**	**0.1**	**41%**
		8	*4*	*2*	*1*	*7*			*2*					*0*				*10*	*0.0*	*12%*

Table 3. Very schematic definition of a standard sequence of diagenetic minerofacies based on data from the Nile Delta, Gulf of Mexico, North Sea, Bay of Bengal, and Nicobar Fan (Milliken, 2007; Morton and Hallsworth, 2007; Andò et al., 2012; Limonta et al., 2018).

ZONE	Association	Indicative depth (km)	Absolute decrease	Relative increase	Relative decrease	Disappearing
0	**Original detrital**	0	----	----	----	----
1	**Hornblende**	< 1	tHMC	hornblende	sillimanite	olivine, clinopyroxene
2	**Epidote-hornblende**	1 - 2	tHMC	epidote	hornblende	sillimanite
3	**Garnet-epidote**	2 - 3	tHMC	garnet	epidote	hornblende
4	**Garnet**	3 - 4	tHMC	ZTR	staurolite, kyanite, titanite	epidote
5	**ZTR**	4 - 5	tHMC	ZTR	garnet	staurolite, kyanite, titanite
6	**ZTR**	5 - 6	tHMC	ZTR	apatite, tourmaline	garnet, chloritoid, monazite
7	**ZTR**	> 6	Extremely depleted assemblages with residual minerals only (ZTR + apatite + Cr-spinel)			

Figure 1. The Nile Delta. The map shows the location of modern beach and dune samples, of pre-Aswan-High-Dam Nile samples provided by the Geological Museum of Fouad I University, and of offshore core samples provided by BP Egypt (Fielding et al., 2018).

Figure 2. The lower Nile course and the Delta. Nile sediments are strongly size-dependent: silty sand carried as suspended load is dominated by volcanic lithics and clinopyroxene, whereas sandy bedload deposited on fluvial bars is progressively enriched in quartz with increasing grain-size, largely because of mixing with coarser quartz-rich eolian sand. All Nile sediments have been trapped in the upper Lake Nubia/Nasser since the closure of the Aswan High Dam, and yet sand composition has not changed much in the Egyptian Nile. In Egypt, eolian supply is limited because the main wind direction is largely parallel to the Nile valley (Hereher, 2010, 2014; Roskin et al., 2014); tributary supply is even much less, and most wadis draining the Red Sea Hills are choked by eolian sand (petrographic and heavy-mineral data after Garzanti et al., 2015). Amp = amphibole; Cpx = clinopyroxene; Ep = epidote; ZTR = zircon + tourmaline + rutile; &tHM = other transparent heavy minerals.

Figure 3. Petrography of Nile Delta sands. **A**) Basaltic detritus carried from Ethiopia before closure of the Aswan High Dam (AHD); **B**) modern beach; **C**) modern backshore dune. Intra-sample variability - with concentration of heavy minerals in the fine tail of the size distribution (125-150 μm class; **above**) and of low-density silicates in the coarse tail (300-355 μm class; **below**) - is a settling-equivalence effect enhanced by mixing with windblown Saharan sand. Inter-sample variability in the lower Pleistocene: **D**) basaltic detritus is common in very fine sand; **E**) subangular to well-rounded quartz predominates in medium sand. **F** to **I**) Older samples are all quartz-rich, but a few felsitic volcanic lithics are invariably present (compare with C_{below}). All photos with crossed polarisers; all blue bars for scale are 50 microns. Q = quartz; K = K-feldspar; P = plagioclase; V =

volcanic lithics (m = mafic; f = felsic); a = amphibole; b = bioclast; m = muscovite; p = clinopyroxene; t = tourmaline.

Figure 4. Petrography of Nile Delta sands (Q = quartz; F = feldspar; L = lithic grains, mostly of volcanic origin). Data are centered to allow better visualization (von Eynatten et al. 2002; Comas-Cufí and Thió-Henestrosa 2011). Volcanic detritus, dominant in silty sand carried as suspended load before closure of the Aswan High Dam (AHD), mixes progressively downstream with quartz-rich eolian sand, which is coarser-grained and thus prevalent in medium-grained sand of the Delta. Grain-size control is indicated also for lower Pleistocene sands (sample ND42 is very fine-grained and lithic-rich, whereas ND41 is medium-grained and quartz-rich) and Pliocene sands. As highlighted by the grey arrow, composition is progressively depleted first in lithic fragments and next in feldspar with age and burial depth. Both fine-grained ND40 and medium-grained ND32 Oligocene samples are pure quartzose sands.

Figure 5. Heavy-mineral dissolution in the Nile Delta succession. For each chronostratigraphic interval, the transparent-heavy-mineral concentration in weight (tHMCw%) is indicated, and for each detrital species the relative abundance and corrosion index [(etched grains + 50% corroded grains) / total grains × 100] are shown in the lower left and right corners of each panel, respectively (definitions as in Andò et al., 2012 and fig. 4 of Nie et al., 2013). Unstable minerals get rapidly leached out down-section. Moderately stable minerals increase their relative abundance in Pliocene strata but are markedly depleted in Miocene strata. Relatively stable minerals - although progressively corroded - increase their relative abundance with increasing age and burial depth.

Figure 6. Down-core compositional trends in Nile Delta sediments. Feldspars (**A**), mafic volcanic and metavolcanic detritus (**B**, **C**), transparent heavy minerals (**D**), and ferromagnesian minerals (**E**; Amp = amphibole, Px = pyroxene; Ol = rare olivine) all decrease exponentially with burial depth,

whereas durable heavy minerals (**F**; ZTR index of Hubert, 1962) relatively increase. Such progressive changes indicate selective intrastratal dissolution rather than provenance control. The marked inter-sample variability of modern sands is related to grain-size control and mixing with quartzose eolian sand along the lower Nile and across the Delta. Note that the degree of heavy-mineral depletion in each stratigraphic interval is the same for sand, sandy silt, and mud samples.

Figure 7. Systematic compositional change with age and burial depth in Nile Delta sediments. **A**) Petrography and heavy minerals in sand; Lvm = volcanic, metavolcanic, and metabasite lithics; Lsm = sedimentary and metasedimentary lithics. **B**) Heavy minerals in sand, sandy silt, and mud. The degree of post-depositional dissolution appears to be only slightly higher in sand than in mud. The volcanic trace inherited from Ethiopian highlands - diluted especially after the closure of the Aswan High Dam (AHD) by mixing with quartz-rich eolian sand along the lower Nile and further across the Delta - becomes fainter in lower Pleistocene sediments, where a few volcanic rock fragments are preserved and pyroxene is rare, and is lost in older sediments by progressive dissolution of less durable minerals. The compositional biplots (Gabriel, 1971) display the relationships among both multivariate observations (points) and mineralogical variables (rays). The length of each ray is proportional to the variability of the parameter in the data set. If the angle between two rays is close to 0°, 90°, and 180°, then the corresponding parameters are directly correlated, uncorrelated, or inversely correlated, respectively. Both biplots combined consistently suggest the following order of mineral durability: olivine < pyroxene < amphibole < epidote < staurolite < titanite < apatite, garnet, AKS (andalusite + kyanite + sillimanite), Cr-spinel, and ZTR (zircon + tourmaline + rutile); tHMC = transparent heavy-mineral concentration.

Figure 8. Comparison between burial-depth distribution of transparent heavy minerals in the Bay of Bengal and Nile Delta (sand and mud samples indicated by red circles and brown squares, respectively). The remarkable similarities of heavy-mineral trends in Cenozoic successions

deposited in orogenic and anorogenic settings indicate overwhelming diagenetic control. Pyroxene virtually disappears at depths of a few tens or hundred of meters, amphibole increases relatively in the first km to be leached out in the second km, where epidote increases at first to disappear next together with titanite and staurolite. Orogenic sediments at depths of 3-4 km are richer in garnet and metamorphic minerals (chloritoid, staurolite, andalusite, kyanite), whereas Cr-spinel, the only stable mineral in mafic and ultramafic rocks, starts to be relatively enriched in anorogenic sediments tapping large igneous provinces as in the Nile case. Minerals still present at depths of 5-6 km include zircon, tourmaline, rutile, apatite, and Cr-spinel. Inset: **A**) the exponential decrease in transparent-heavy-mineral concentration and grain density (correlation coefficients up to 0.82 for offshore Nile Delta sand) provides independent evidence for downward increasing heavy-mineral dissolution with burial depth. Ol = olivine; Px = pyroxene; Amp = amphibole; Ep = epidote; Ttn = titanite; St = staurolite; Grt = garnet; AKS = andalusite + kyanite + sillimanite; Cld = chloritoid; Mon = monazite; Ap = apatite; Tur = tourmaline; Sp = Cr-spinel; Rt = rutile; Zrn = zircon.

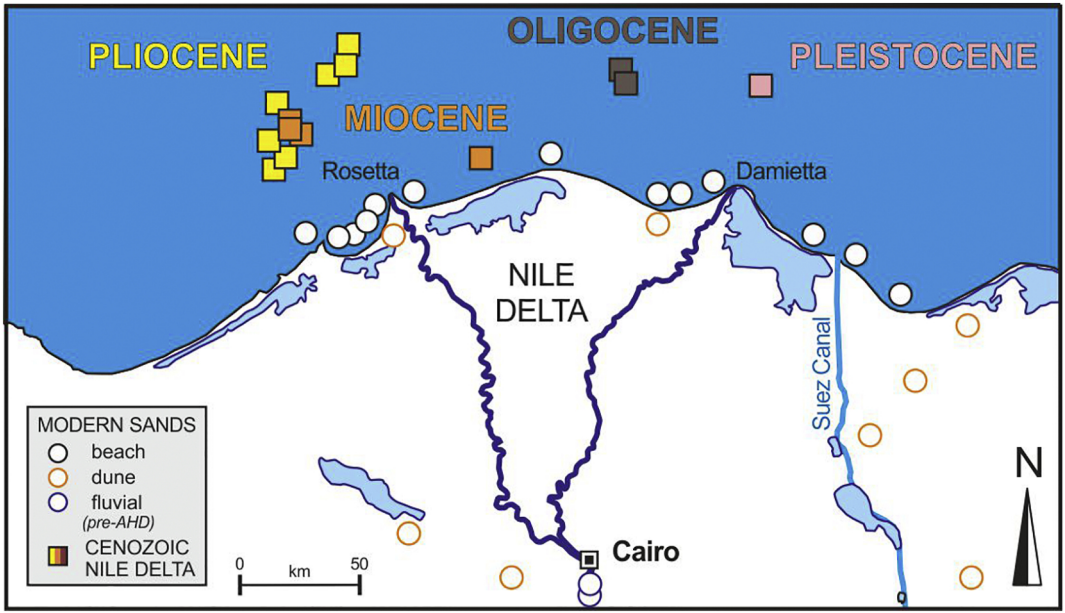
PLIOCENE
OLIGOCENE
PLEISTOCENE
MIOCENE
Rosetta
Damietta
NILE
DELTA
Suez Canal
MODERN SANDS
beach
dune
fluvial
(pre-AHD)
CENOZOIC
NILE DELTA
0
km
50
Cairo
N

Figure 1


longest fetch direction
MEDITERRANEAN SEA
Nile littoral cell
Dead Sea
main wind direction
Cairo
Fayyum
SINAI
WESTERN DESERT
Wadi Qena
RED SEA
RED SEA HILLS
EGYPT
Aswan High Dam
Lake Nubia / Nasser
SUDAN
NILE RIVER SEDIMENTS
Silty sand
Fine sand
Medium sand
Key
heavy minerals
&HM
ZTR
quartz
Ep
Amp
Cpx
feldspar
volcanic lithics
& lithics
+ mica

Figure 2

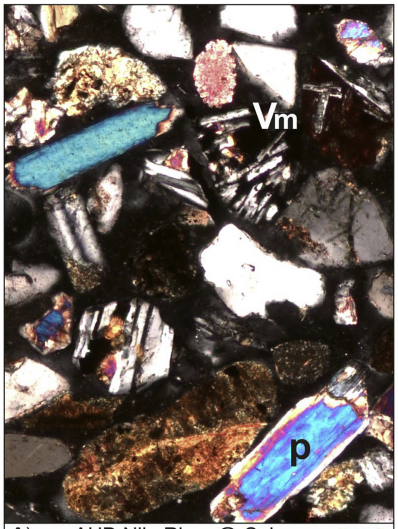

A) pre-AHD Nile River @ Cairo

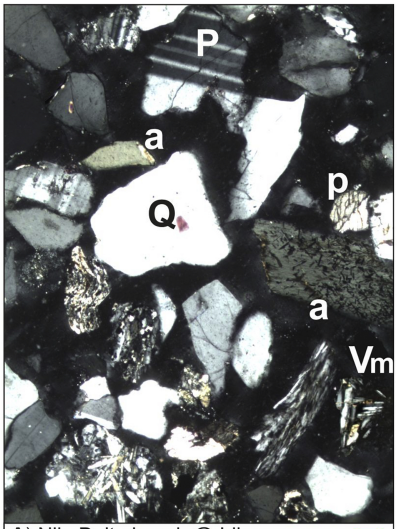

A) Nile Delta beach @ Idku

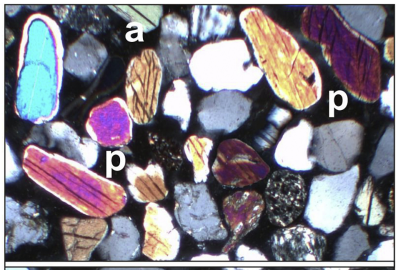

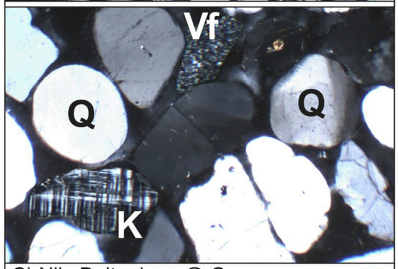

C) Nile Delta dune @ Gamasa

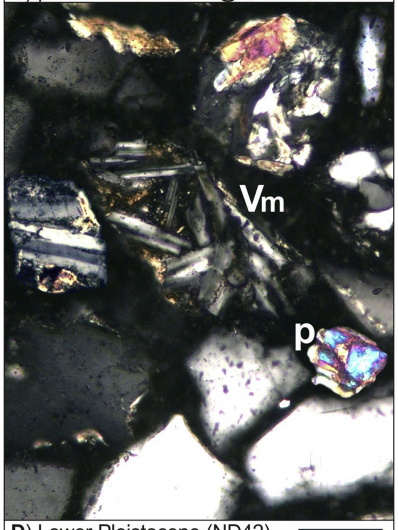

D) Lower Pleistocene (ND42)

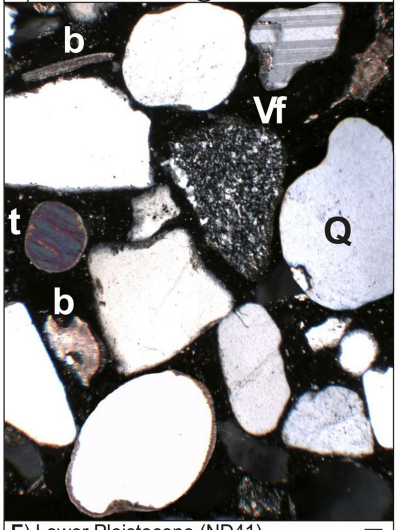

E) Lower Pleistocene (ND41)

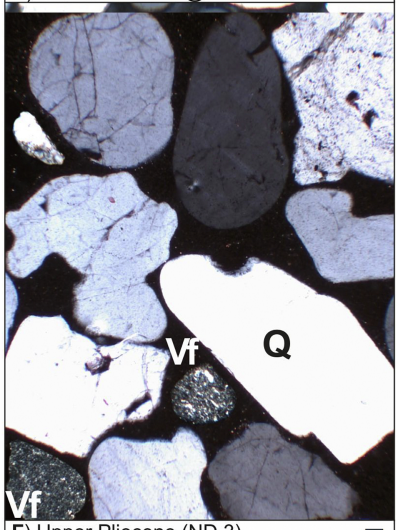

F) Upper Pliocene (ND 3)

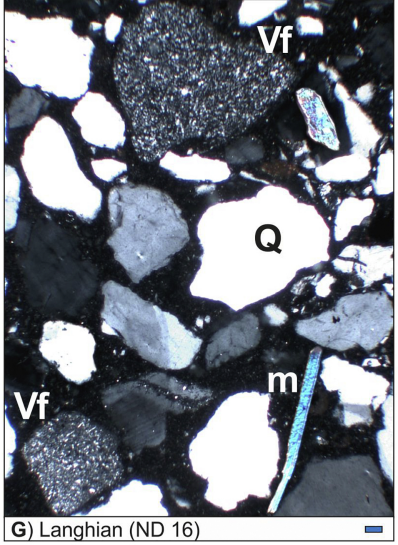

G) Langhian (ND 16)

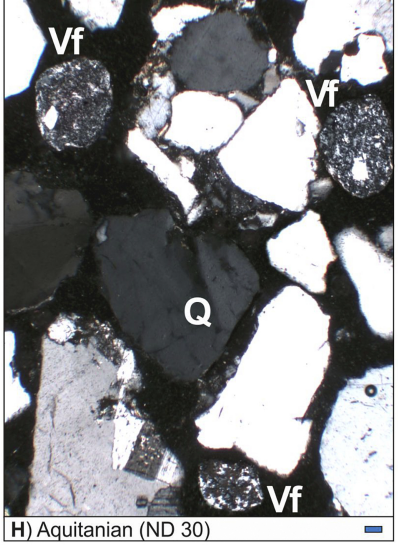

H) Aquitanian (ND 30)

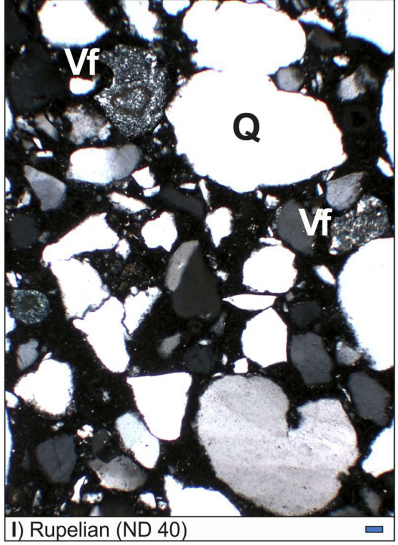

I) Rupelian (ND 40)

Figure 3

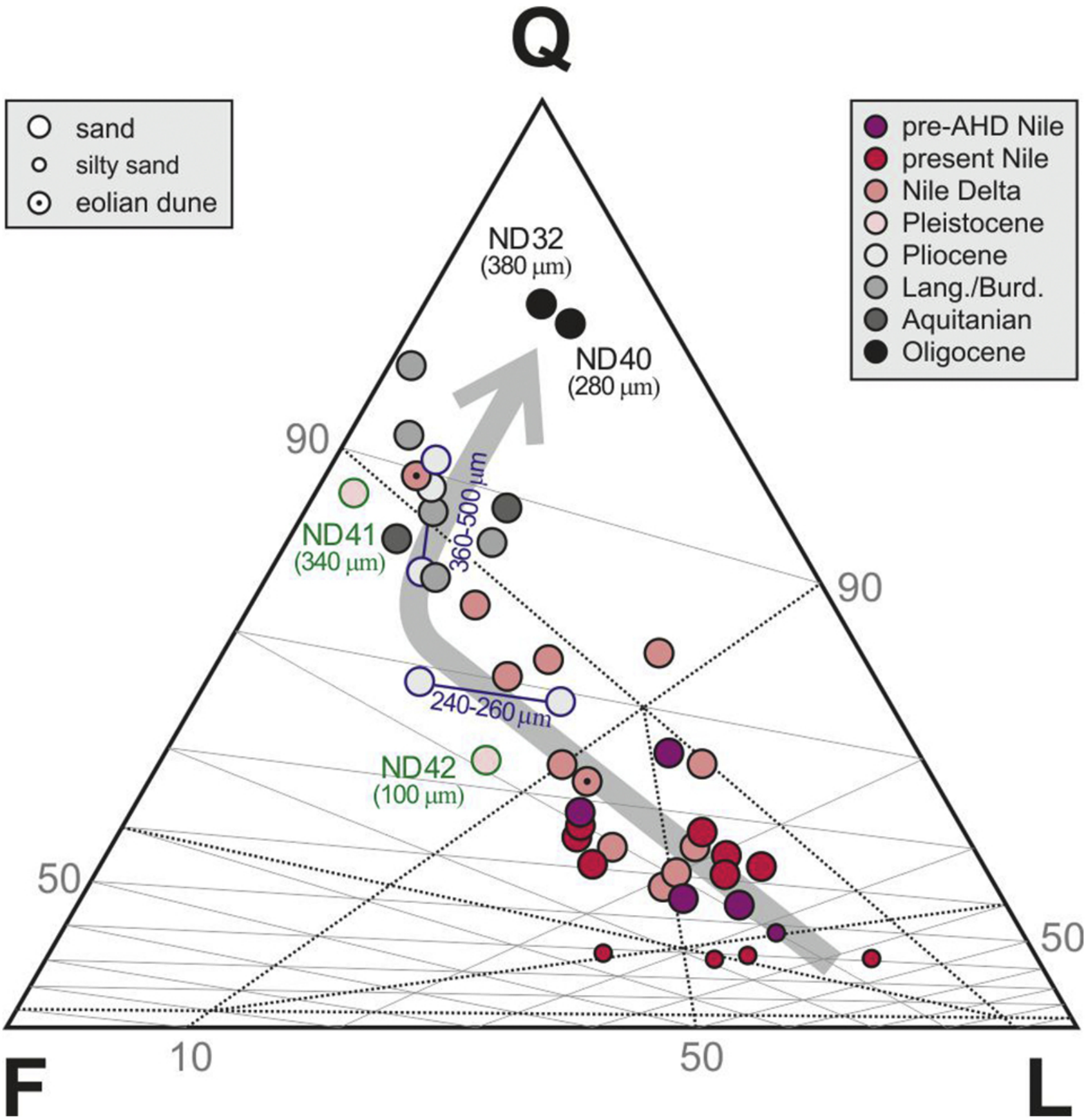
Q
F
L
sand
silty sand
eolian dune
pre-AHD Nile
present Nile
Nile Delta
Pleistocene
Pliocene
Lang./Burd.
Aquitanian
Oligocene
ND32
(380 μm)
ND40
(280 μm)
ND41
(340 μm)
ND42
(100 μm)
360-500 μm
240-260 μm
90
90
50
50
10
50

Figure 4

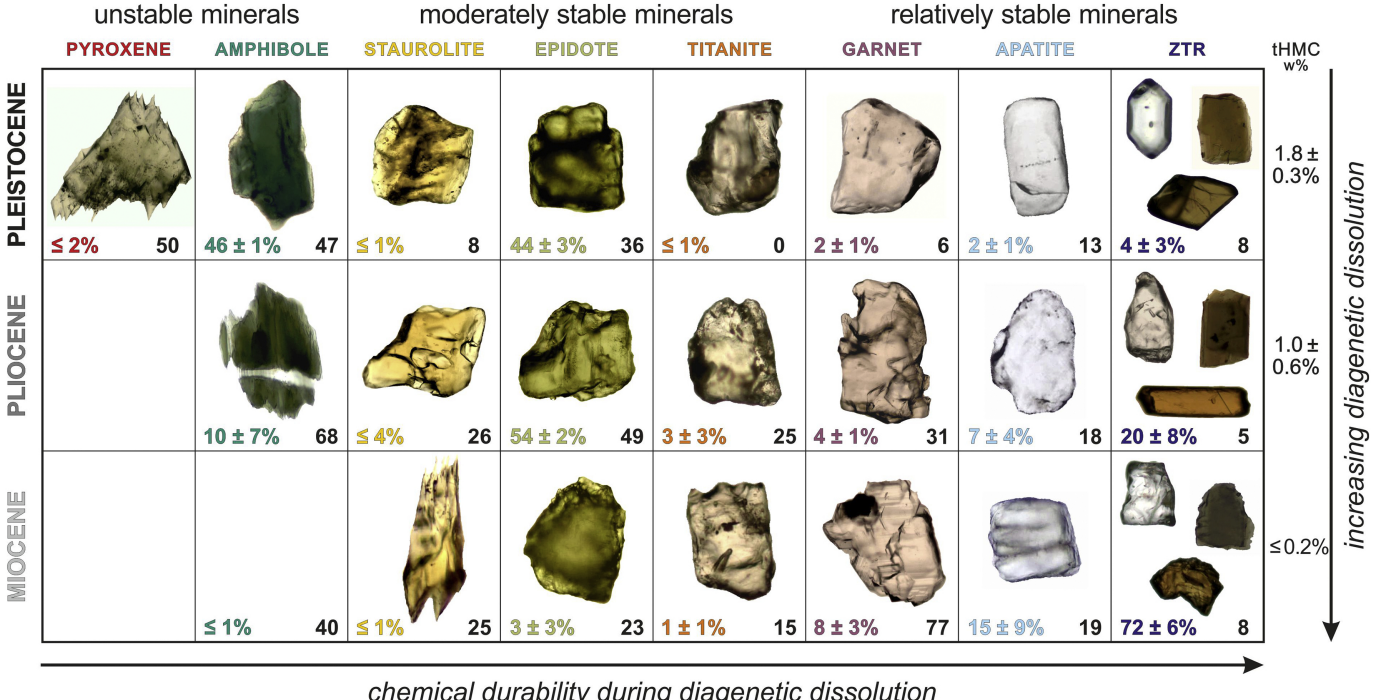
unstable minerals
moderately stable minerals
relatively stable minerals
PYROXENE
AMPHIBOLE
STAUROLITE
EPIDOTE
TITANITE
GARNET
APATITE
ZTR
tHMC w%
PLEISTOCENE
PLIOCENE
MIOCENE
≤ 2% 50
46 ± 1% 47
≤ 1% 8
44 ± 3% 36
≤ 1% 0
2 ± 1% 6
2 ± 1% 13
4 ± 3% 8
1.8 ± 0.3%
10 ± 7% 68
≤ 4% 26
54 ± 2% 49
3 ± 3% 25
4 ± 1% 31
7 ± 4% 18
20 ± 8% 5
1.0 ± 0.6%
≤ 1% 40
≤ 1% 25
3 ± 3% 23
1 ± 1% 15
8 ± 3% 77
15 ± 9% 19
72 ± 6% 8
≤ 0.2%
increasing diagenetic dissolution
chemical durability during diagenetic dissolution

Figure 5

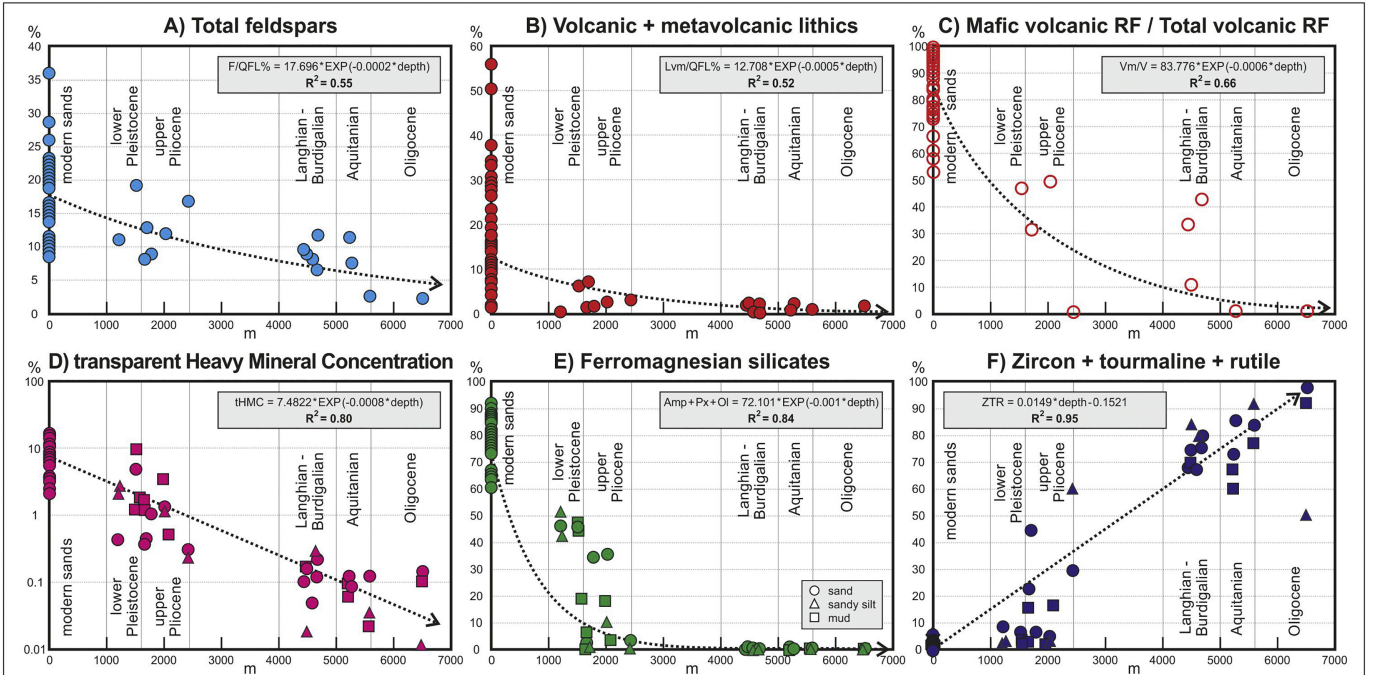
A) Total feldspars
F/QFL% = 17.696*EXP(-0.0002*depth)
R² = 0.55
B) Volcanic + metavolcanic lithics
Lvm/QFL% = 12.708*EXP(-0.0005*depth)
R² = 0.52
C) Mafic volcanic RF / Total volcanic RF
Vm/V = 83.776*EXP(-0.0006*depth)
R² = 0.66
D) transparent Heavy Mineral Concentration
tHMC = 7.4822*EXP(-0.0008*depth)
R² = 0.80
E) Ferromagnesian silicates
Amp+Px+Ol = 72.101*EXP(-0.001*depth)
R² = 0.84
F) Zircon + tourmaline + rutile
ZTR = 0.0149*depth-0.1521
R² = 0.95
modern sands
lower Pleistocene
upper Pliocene
Langhian - Burdigalian
Aquitanian
Oligocene
sand
sandy silt
mud
%
m

Figure 6

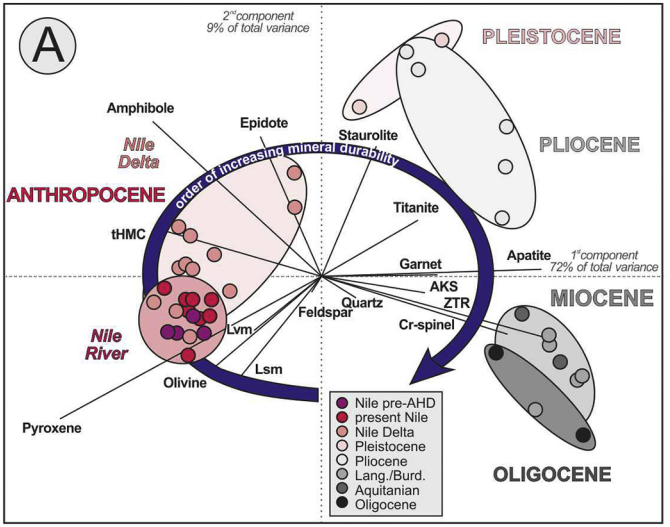
A
2nd component
9% of total variance
PLEISTOCENE
PLIOCENE
MIOCENE
OLIGOCENE
ANTHROPOCENE
Nile Delta
Nile River
order of increasing mineral durability
Amphibole
Epidote
Staurolite
Titanite
Apatite
Garnet
AKS
ZTR
Cr-spinel
Quartz
Feldspar
tHMC
Lvm
Lsm
Olivine
Pyroxene
1st component
72% of total variance
Nile pre-AHD
present Nile
Nile Delta
Pleistocene
Pliocene
Lang./Burd.
Aquitanian
Oligocene

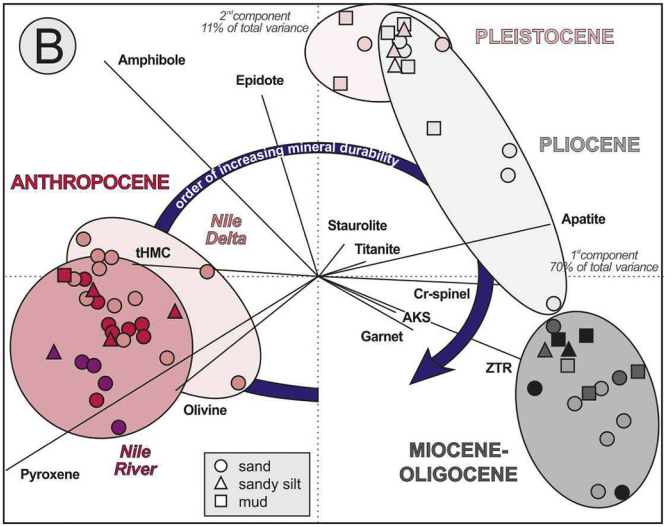
B
2nd component
11% of total variance
PLEISTOCENE
PLIOCENE
MIOCENE-
OLIGOCENE
ANTHROPOCENE
Nile Delta
Nile River
order of increasing mineral durability
Amphibole
Epidote
Staurolite
Titanite
Apatite
Garnet
AKS
Cr-spinel
ZTR
tHMC
Olivine
Pyroxene
1st component
70% of total variance
sand
sandy silt
mud

Figure 7

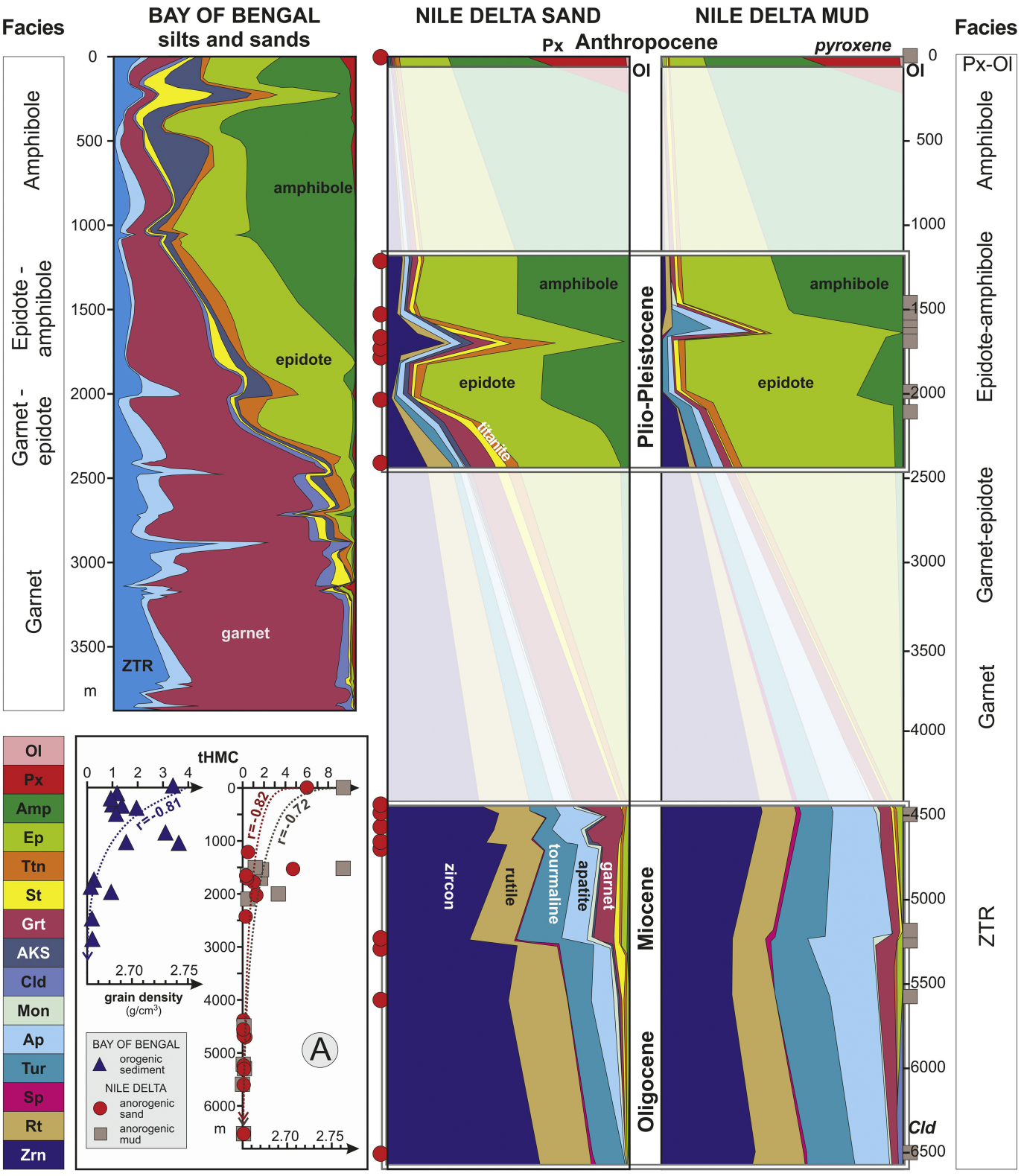
Facies
BAY OF BENGAL
silts and sands
NILE DELTA SAND
NILE DELTA MUD
Facies
Px
Anthropocene
pyroxene
Ol
Px-Ol
Amphibole
Epidote - amphibole
Garnet - epidote
Garnet
amphibole
epidote
garnet
ZTR
titanite
Plio-Pleistocene
Miocene
Oligocene
zircon
rutile
tourmaline
apatite
garnet
Cld
m
0
500
1000
1500
2000
2500
3000
3500
4000
4500
5000
5500
6000
6500
Ol
Px
Amp
Ep
Ttn
St
Grt
AKS
Cld
Mon
Ap
Tur
Sp
Rt
Zrn
tHMC
r=-0.81
r=-0.82
r=-0.72
2.70
2.75
grain density
(g/cm3)
BAY OF BENGAL
orogenic sediment
NILE DELTA
anorogenic sand
anorogenic mud
A

Figure 8